Association Patterns in $(HF)_m(H_2O)_n$ ($m + n = 2-8$) Clusters

Barath Baburao,[†] Donald P. Visco, Jr.,*[,†] and Titus V. Albu*[,‡]

Department of Chemical Engineering, Tennessee Technological University, Box 5013, and Department of Chemistry, Tennessee Technological University, Box 5055, Cookeville, Tennessee 38505

Received: April 9, 2007; In Final Form: May 25, 2007

In an attempt to understand the phase behavior of aqueous hydrogen fluoride, the clustering in the mixture is investigated at the molecular level. The study is performed at the mPW1B95/6-31+G(d,p) level of theory. Several previous studies attempted to describe the dissociation of HF in water, but in this investigation, the focus is only on the association patterns that are present in this binary mixture. A total of 214 optimized geometries of $(HF)_n(H_2O)_m$ clusters, with $m + n$ as high as 8, were investigated. For each cluster combination, several different conformations are investigated, and the preferred conformations are presented. Using multiple linear regressions, the average strengths of the four possible H-bonding interactions are obtained. The strongest H-bond interaction is reported to be the $H_2O\cdots H-F$ interaction. The most probable distributions of mixed clusters as a function of composition are also deduced. It is found that the larger $(HF)_n(H_2O)_m$ clusters are favored both energetically and entropically compared to the ones that are of size $m + n \leq 3$. Also, the clusters with equimolar contributions of HF and H_2O are found to have the strongest interactions.

1. Introduction

The phase behavior of aqueous hydrogen fluoride has been studied since the late 1940s. Munter and co-workers[1] reported an azeotrope for this system with a composition of 38.26 wt % HF and a maximum boiling temperature of 385 K at 1 atm. The presence of such an extreme negative azeotrope indicates the existence of strong attractive forces between the components in the mixture.[2] The strong interactions between the HF and water, called the cross-association, and the strength of HF's own self-association interactions are also responsible for the relative weak acidity of hydrofluoric acid compared to the other hydrohalic acids.[3−5] Due to the extreme corrosive nature of HF in both anhydrous and aqueous forms, an experimental determination of phase equilibrium properties of this mixture is inconvenient and difficult.

Modeling the HF−water mixture has been proven to be difficult as well. When an advanced thermodynamic model[6] was used for this particular mixture, a very large binary interaction parameter value was required to correlate the phase coexistence properties at 1 atm. This is mainly because of the deficiency of the model in incorporating the strong HF−water interactions. Such complex interactions in this system are also reinforced by the evaluation[7] of the thermodynamic consistency of three experimental data sets available for this mixture at 1 atm[1,8,9] and also from molecular simulation studies[10] on this mixture. Both approaches indicate that the dilute HF and dilute water regions of this mixture may result in unusual infinite dilution fugacity coefficients and a fluorophobic-like effect, which only goes toward providing more evidence as to the complexity of this mixture and the modeling challenges this system possesses.

In order to develop a robust, accurate, and predictive bulk-phase thermodynamic model describing the properties of the mixture, one has to properly account for associative interactions in both the pure components as well as in the mixture. Both water and hydrogen fluoride show distinct multidimensional hydrogen bond (H-bond) networks.[11] So when these pure components are mixed, the potential association patterns in the mixture could be quite complex. To our knowledge, the association patterns in the HF−H_2O system are yet to be determined experimentally. There are just a few theoretical studies that have attempted to answer the structural properties of this mixture,[12−15] and none address both the self-and the cross-association patterns. Also, most of these studies are mainly devoted to understanding the interaction within the smaller clusters, $(HF)_m(H_2O)_n$, with $m + n \leq 3$. Studies on the larger clusters are mostly focused on the dissociation chemistry of one HF molecule in the mixture.[4,16−20]

Many thermodynamic modeling approaches for strongly associating systems focus on the proper capturing of the association interactions within the system.[21−25] Accordingly, the selection of the association scheme to be used is quite important. In HF, several association schemes for just the pure component utilize large oligomer sizes, even up to the 12-mer.[26] Obviously, when designing an association scheme for the aqueous HF system, this creates many options as to what to include in the scheme. For example, there are 28 unique cross associates up to eight molecules that can be formed from HF and water. This, in turn, leads to 268 million unique association schemes that one can imagine. Therefore, it is prudent from a modeling standpoint to try to focus only on those oligomers that are most likely to occur. Hence, in this work, we investigate the association patterns using cluster models in order to identify the cross-association patterns that are likely to be found in solution and that should be included in bulk-phase thermodynamic modeling of the aqueous HF system. We studied these association patterns in the hydrogen fluoride-water mixture using $(HF)_m(H_2O)_n$ clusters with sizes, $m + n$, of up to eight molecules. We also investigated the expected existence of the clusters in

* To whom correspondence should be addressed. D.P.V.: e-mail, dvisco@tntech.edu; phone, 931-372-3606; fax, 931-372-6352. T.V.A.: e-mail, albu@tntech.edu.
[†] Department of Chemical Engineering.
[‡] Department of Chemistry.

10.1021/jp0727648 CCC: $37.00
Published on Web 07/17/2007

solution as a function of the concentration of hydrogen fluoride in the mixture.

This paper is ordered as follows. First, we provide some computational details of the methodology used. We report the results for pure hydrogen fluoride and water, then the results for the cross-associate clusters. These are reported with increasing cluster size defined by the number of molecules in the cluster. We then discuss the strength of various types of hydrogen bonds present in the mixture and the stabilities of possible types of cross associates depending on the mixture composition. We finalize the paper with the conclusions of the study.

2. Computational Methodology

The electronic structure calculations were carried out at the mPW1B95/6-31+G(d,p) level of theory.[27−30] The mPW1B95 is a newly developed, one-parameter hybrid meta density functional theory method that utilizes Adamo and Barone's mPW exchange functional and Becke's B95 correlation functional, with a contribution of 31% Hartree−Fock exchange functional. We choose the mPW1B95 functional for this study because it is computationally affordable for the size and the number of systems investigated here, and also because it was shown by Zhao and Truhlar[27] to be accurate in predicting the energetics of nonbonding interactions. The geometry optimizations were carried out using a tight convergence criterion and the default integration grid for numerical integrations. The electronic spin multiplicity is 1 for all investigated systems, and the calculations were done using restricted wave functions. All optimized minima were characterized by all positive normal-mode frequencies. In the thermochemistry analysis, we used rigid rotor−harmonic oscillator approximation. All the electronic structure theory calculations were carried out using the *Gaussian*03 software.[31]

3. Results

Throughout this work, each cluster, both the pure components and the mixture, is named based on the number of HF molecules and number H_2O molecules present in the cluster. The relative stabilities of various optimized structures were determined based on the energetics of the cluster formation from separated constituting molecules:

$$m\mathrm{HF} + n\mathrm{H_2O} \rightarrow (\mathrm{HF})_m(\mathrm{H_2O})_n \qquad (1)$$

This process is a measure of the binding intermolecular (i.e., H-bond) interactions in the cluster and is characterized, in this study, by the zero-point-exclusive (i.e., electronic) energy of reaction, denoted ΔE, the zero-point-inclusive energy of reaction (equal to the enthalpy of reaction at 0 K), denoted ΔH_0, and the Gibbs free energy of reaction at 298.15 K and 1 atm, denoted ΔG_{298} or just ΔG. We choose to consider all three values in interpreting the results because the value of ΔG is strongly dependent on the calculated vibrational frequency values, especially the low-frequency values. This can introduce a certain degree of uncertainty in our results; uncertainty that is not present in the ΔE value or is not very significant in the ΔH_0 value.

The clusters are described as dimers, trimers, etc., based on the number of molecules that form them (i.e., the $m + n$ value). For almost all $(HF)_m(H_2O)_n$ clusters, we determined more than a single optimized structure. These different (electronic) energy minima are called conformations and are labeled as $m-n-X$ where m and n are the number of HF and H_2O molecules in the cluster, respectively, and X is a letter, starting from A, ranking the stability of these clusters based on the calculated ΔE values. For example, the lowest energy (i.e., the most negative ΔE value) pure HF hexamer is labeled 6−0−A. In most cases, we only present representative structures in the discussion, in figures and in tables, but all un-ionized structures (and only the un-ionized structures) were considered in analyzing the data. Note also that only the un-ionized structures were labeled according to the rule above. (An ionized structure is one in which one molecule of HF ionized to form H_3O^+ and F^- ions.) The geometries of all optimized structures are given as Supporting Information.

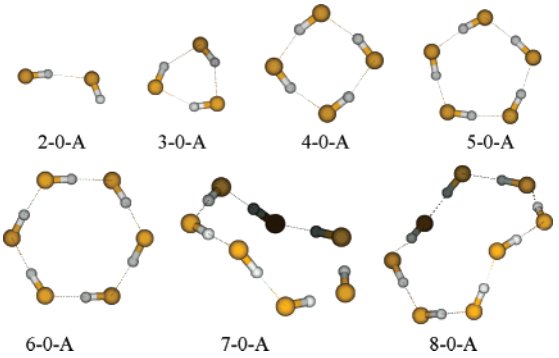

Figure 1. Representative geometries of $(HF)_{2-8}$ clusters.

TABLE 1: Binding Energies of Selected Conformations of $(HF)_{2-8}$ Clusters with and without Zero-Point Energy Contributions as Well as the Gibbs Free Energy at $T = 298.15$ K and $P = 1$ atm[a]

conformation	ΔE	ΔH_0	ΔG
2−0−A	−5.00	−3.21	2.12
3−0−A	−16.15	−11.29	2.17
4−0−A	−29.60	−22.25	−0.73
5−0−A	−40.96	−31.59	−2.76
6−0−A	−50.63	−39.40	−3.20
7−0−A	−59.80	−46.64	−3.51
8−0−A	−68.78	−53.72	−3.20

[a] All values are in kcal/mol.

3.1. $(HF)_m$ Clusters. Ever since the gas-phase thermodynamic properties and structures of HF were studied by Redington,[26] numerous experimental[32−43] and theoretical[41,44−61] studies on HF clusters have been reported. Extensive data on the enthalpy and entropy of HF clusters derived from various studies have been complied in the JANAF tables.[62] These studies indicate the existence of a significant concentration of dimers and hexamers and relatively low concentrations of trimers, tetramers and pentamers as well.[47] Even though the existence of higher order oligomers of sizes more than hexamer are reported,[26,49,62] the structural data is present only for bent chain dimers[63] and cyclic hexamers.[32] Previous theoretical studies on the HF dimer indicate that the bent chain structure, having only one strong hydrogen bond, is more stable than a cyclic structure, having two formal hydrogen bonds. For the larger $(HF)_m$ clusters, with $m = 3-6$, planar cyclic nonpolar structures were reported to be the most stable ones,[47,51] while for $m = 7, 8$ nonplanar cyclic structures were reported to be the most stable ones.[52]

The optimized structures of $(HF)_m$ with $m = 2-8$ obtained in this study are shown in Figure 1, and the binding energies of these clusters are given in Table 1. The mPW1B95/6-31+G(d,p) structures for pure HF clusters are in good agreement with the optimized structures reported previously.[47,51,52] Also, the F···F distance for the dimer, 2.74 A, and the average F···F distance in the 6−0−A hexamer, 2.46 A, are in good agreement

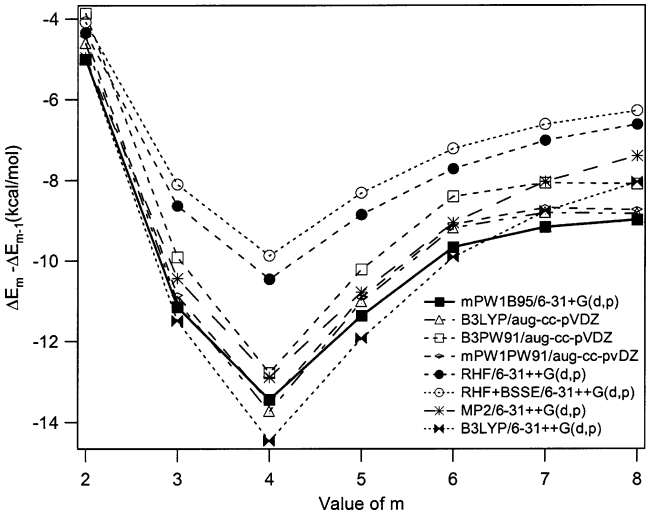

Figure 2. Stepwise binding energy in kcal/mol vs the cluster size for $(HF)_{2-8}$ clusters.

with the gas-phase experimental distances of 2.72[34] and 2.53 A,[64] respectively. The ΔE and ΔH_0 values given in Table 1 for $(HF)_2$ are in good agreement with the experimental values of −4.63 and −3.03 kcal/mol, respectively.[33]

It is known that H-bond aggregates show non-additive cooperative effects due to many body interactions.[47,65] In other words, the formation of a hydrogen bond results in a change of charge distribution in such a way that the hydrogen acceptor becomes potentially a better H-bond donor than the non-H-bonded HF and vice versa.[66] Accordingly, the formation of the first H-bond enhances the formation of the second H-bond and so on. Figure 2 shows the non-additive cooperative effect in HF clusters that is found in this work (solid line) in comparison with earlier studies[47,51,52] that are reported at various other levels of theory. The stepwise binding energy is shown as a function cluster size. Similar to previous studies,[47,51,52,67] it can be seen that a strong non-additive cooperative effect is observed when moving from dimer to trimer and tetramer. This effect decreases until the hexamer, and eventually, it reaches a constant value near the octamers. Due to this cooperative effect, it is not surprising that the geometrical parameters vary from one-cluster to other, and this is present for both the pure components and the binary mixture. For instance, the F···F distance, a measure of the distance between the molecules in the cluster, changes from 2.74 A in the 2−0−A dimer to an average of 2.45 A in the 8−0−A octamer, which is almost a 10% reduction. As another indication of the strength of the interaction between the HF molecules, the H−F bond length increase (being elongated due to H-bond interactions) from an average of 0.924 A in the 2−0−A dimer to an average of 0.961 A in the 8−0−A octamer.

At the mPW1B95/6-31+G(d,p) level of theory, for pure HF, the Gibbs free energies at 298 K and 1 atm given in Table 1 indicate that the most stable cluster, compared to HF monomers, is the heptamer. This result is different than the one obtained at the MP2/6-31++G(d,p) level of theory, for which the hexamer was found to be the most stable cluster. In comparison with earlier work on HF clusters,[47] it can be seen that the level of theory in this study predicts stronger binding energies than restricted Hartree−Fock and MP2 methods and weaker binding energies than the one obtained using B3LYP method, all these methods being used with the 6-31++G(d,p) basis set.[47] Nevertheless, in all cases, the one-ring, cyclic structure is found to be the most stable conformation for HF *i*-mer ($i = 3-8$), which is in good agreement with the earlier studies on this cluster.[47,51,52]

3.2. $(H_2O)_n$ Clusters. A large number of studies have been carried out on the structural properties of water clusters using various theoretical as well as experimental methods. For detailed reviews on these developments, we refer the reader elsewhere.[66,68−72] The focus of the current study, with respect to the water clusters, is merely to determine the binding energies for the known water clusters at the same level of theory as the cross clusters. The optimized structures of $(H_2O)_n$ with $n = 2-8$ are shown in Figure 3, and the binding energies are given in Table 2. For cluster sizes up to 5, the same conformation has both the lowest electronic energy and the lowest Gibbs free energy. However, when the cluster size is increased, the entropic term plays a more significant role, and the conformation of minimum electronic energy is not necessarily the same as the one of minimum Gibbs free energy. As a result, in Figure 3, we have reported the structures of minimum ΔE and ΔG for each cluster.

Owing to its accessibility and size, the water dimer is perhaps the most thoroughly studied H-bonded system known and boasts many experimental[73−79] and theoretical investigations.[80−93] The O···O distance in the water dimer calculated at mPW1B95/6-31+G(d,p) level of theory is 2.89 A, in fair agreement with the measured value of 2.976 A.[74,75] The binding energy for the dimer calculated in this study, 6.07 kcal/mol, is also in good agreement with the experimental value of 5.5 ± 0.7 kcal/mol.

Even though earlier vibrational spectroscopy[94] as well as ab initio[95] studies suggested a nearly linear open-chain structure for $(H_2O)_3$, the most stable arrangement for the trimer was found to be a cyclic structure with a C_1 symmetry,[68] and the $(H_2O)_3$ structure in this work is in agreement with this previous finding. For $(H_2O)_4$, three different optimized structures were considered, with the most stable structure having an almost square planar arrangement (determined by the position of the oxygen atoms), similar to reported structures from earlier studies.[69,81,84,85,88,92,93,96−99] For $(H_2O)_5$, four different stable structures were determined. Similar to the trimer and tetramer, the most stable structure has a cyclic pattern, with the shape of an almost planar pentagon. The other three structures determined for water pentamer are nonplanar, with cage, spiral and book conformations.[69]

The $(H_2O)_6$ cluster is generally considered to represent an important class of water clusters as it marks the transition to 3-dimensional arrangements.[100] Earlier studies indicate the existence of both cyclic[66,85,87,88,100−103] as well as alternative 3-dimensional structures such as chair, boat, and cage conformations.[69,104−112] In our study, eight different minimum-energy structures were determined for $(H_2O)_6$. Even though the prism structure, 0−6−A, is energetically preferred, the cyclic (chair) structure, 0−6−C is entropically favored (leading to a smaller ΔG value). While considering the electronic energy only, the prism structure is favored by 0.19 kcal/mol. On the other hand, the relative Gibbs free energy difference at 298 K is about 4.29 kcal/mol in favor of the cyclic structure. For the $(H_2O)_7$ system, five different optimized structures were considered, with the preferred structure based on ΔE values having a cage-like structure (0−7−A structure in Figure 3), similar to earlier studies.[98,113−117] However, the cyclic chair conformation (0−7−E structure in Figure 3) is entropically favored. Here, the cage structure is favored by around 4.83 kcal/mol considering only the ΔE values, and the cyclic chair conformation is favored by 2.96 kcal/mol when comparing the ΔG values.

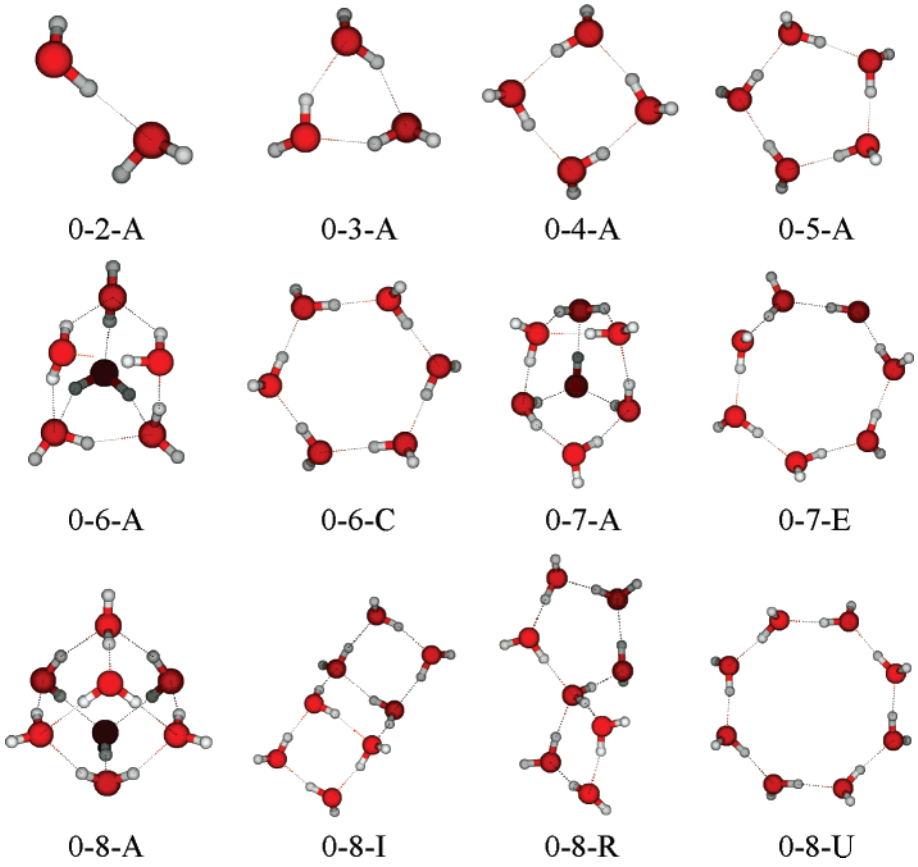

Figure 3. Representative geometries of $(H_2O)_{2-8}$ clusters.

TABLE 2: Binding Energies of Selected Conformations of $(H_2O)_{2-8}$ Clusters with and without Zero-Point Energy Contributions as Well as the Gibbs Free Energy at $T = 298.15$ K and $P = 1$ atm[a]

conformation	ΔE	ΔH_0	ΔG
0−2−A	−6.07	−3.70	2.11
0−3−A	−18.24	−12.37	2.53
0−4−A	−31.83	−22.76	0.88
0−5−A	−41.88	−30.90	0.38
0−6−A	−52.12	−37.31	4.71
0−6−C	−51.93	−38.76	0.42
0−7−A	−64.77	−46.89	4.25
0−7−E	−59.93	−44.90	1.32
0−8−A	−81.15	−59.62	2.68
0−8−I	−76.55	−55.65	5.22
0−8−R	−71.02	−52.37	3.52
0−8−U	−68.80	−51.75	2.15

[a] All values are in kcal/mol.

Earlier studies[69,88,98,108,118−121] on $(H_2O)_8$ indicate that the cube-like structures are the lowest-energy ones for this cluster. Belair and Francisco[121] reported 14 topologically different stable cubic $(H_2O)_8$ structures. While the stability of the cubic structures is well established, it changes at higher temperatures. Kim et al.[118] reported the cyclic structures to be the most stable $(H_2O)_8$ cluster at room temperature, whereas Mrázek et al.[69] reported recently that the cubic structure to be the most stable at the same temperature. In this work, we considered 20 different optimized geometries for the $(H_2O)_8$ cluster. Similar to Kim et al.,[118] we found the cyclic structure to be entropically favored when compared to the cubic structures, which are energetically favored. For the water octamer, the cubic structure 0−8−A is favored by around 12.30 kcal/mol comparing the ΔE values, and the cyclic structure, 0−8−U, is favored by 0.50 kcal/mol comparing the ΔG values. Some additional interesting structures, 0−8−I and 0−8−R, are also shown in Figure 3.

3.3. Cross Clusters. Previous sections describe various structures obtained for both pure HF and pure H_2O. In this section, we present the optimized structures that were obtained for $(HF)_m(H_2O)_n$clusters. The structures are discussed as the cluster size increases from dimer to octamer. For each *i*-mer, where $i = m + n$, every possible combination of cross-associate clusters are presented. The binding energies for representative $(HF)_m(H_2O)_n$ cluster structures are given in Table 3.

3.3.1. Dimer. $(HF)_1(H_2O)_1$. The most stable structure for the HF−H_2O cluster, 1−1−A, is shown in Figure 4. The binding energies obtained for this HF−H_2O cluster are in good agreement with the experimental values of $\Delta H_0 = -8.2$ kcal/mol and $\Delta E = -10.25$ kcal/mol.[122] The calculated O···F distance, 2.64 A, is also in good agreement with the experimental value of 2.66 A.[123] The F−H···O angle is almost linear at 177.8 degrees, in agreement with the previous theoretical result obtained at the B3LYP/D95++(p,d) level of theory.[4] The H-bond distance (i.e., the distance between the H atom in HF and O atom in H_2O) is 1.71 A, which is 0.08 A less than the H-bond distance in $(H_2O)_2$ and 0.133 A less than that of $(HF)_2$.

3.3.2. Trimers. $(HF)_1(H_2O)_2$ and $(HF)_2(H_2O)_1$. In Figure 4, 1−2−A and 2−1−A are the most stable structures for these two cross clusters. Both these structures are cyclic with comparable bond distances. The H-bond distance between the hydrogen of HF and the oxygen of the closest water, $R(H_2O\cdots HF)$, is 1.66 A in the $(HF)_1(H_2O)_2$ cluster and 1.57 A in the $(HF)_2(H_2O)_1$ cluster. Both these values are shorter than the distance in the $(HF)_1(H_2O)_1$ cluster, which is 1.71 A. The H−F bond length in the HF molecule closest to the H_2O molecule is elongated in both clusters, 0.957 A for $(HF)_1(H_2O)_2$ and 0.961 A for $(HF)_2(H_2O)_1$, in comparison with the 0.926 A

TABLE 3: Binding Energies of Selected Conformations of $(HF)_m(H_2O)_n$ Clusters ($m + n = 2-8$) with and without Zero-Point Energy Contributions as Well as the Gibbs Free Energy Changes at $T = 298.15$ K and $P = 1$ atm[a]

conformation	ΔE	ΔH_0	ΔG	conformation	ΔE	ΔH_0	ΔG	conformation	ΔE	ΔH_0	ΔG
1−1−A	−10.21	−7.40	−1.36	3−3−C	−58.60	−45.62	−6.80	1−7−L	−66.13	−47.62	8.59
1−2−A	−20.74	−15.07	−0.63	4−2−A	−58.84	−46.98	−10.57	2−6−A	−85.22	−64.89	−4.70
2−1−A	−20.21	−14.81	−0.81	4−2−C	−56.47	−43.98	−5.86	2−6−B	−79.72	−60.50	−3.01
1−3−A	−34.07	−25.67	−2.90	4−2−D	−52.05	−39.58	−1.72	2−6−E	−78.84	−60.72	−5.35
1−3−B	−28.34	−20.89	0.40	5−1−A	−55.30	−43.84	−7.37	2−6−F	−77.35	−59.60	−4.59
2−2−A	−36.06	−27.78	−5.12	5−1−C	−50.23	−39.63	−4.22	2−6−I	−76.24	−59.29	−7.29
2−2−B	−35.07	−26.93	−4.28	5−1−D	−46.50	−34.92	3.49	3−5−A	−85.83	−66.53	−7.10
3−1−A	−33.93	−26.16	−4.04	1−6−A	−67.03	−50.09	−0.34	3−5−B	−82.46	−64.63	−9.26
1−4−A	−45.85	−34.98	−3.88	1−6−B	−64.60	−48.94	−0.99	3−5−C	−80.91	−62.21	−5.32
1−4−B	−43.27	−32.10	−0.48	1−6−E	−63.20	−48.69	−1.70	3−5−D	−80.30	−62.33	−6.98
1−4−G	−40.97	−30.75	−1.00	2−5−A	−69.19	−53.73	−6.12	3−5−G	−78.93	−62.16	−9.60
2−3−A	−48.29	−37.72	−7.12	2−5−D	−67.43	−52.70	−7.51	4−4−A	−85.89	−67.12	−8.16
2−3−B	−43.65	−33.43	−2.76	2−5−E	−66.60	−50.71	−3.16	4−4−B	−81.48	−62.98	−6.29
2−3−C	−42.50	−32.64	−3.34	3−4−A	−70.13	−54.09	−5.09	4−4−C	−81.46	−63.77	−8.98
3−2−A	−48.42	−38.24	−8.10	3−4−B	−69.68	−55.10	−9.78	4−4−D	−81.28	−64.76	−13.32
3−2−B	−46.88	−36.89	−6.81	3−4−C	−68.53	−52.73	−5.36	4−4−E	−80.25	−62.06	−5.83
4−1−A	−45.54	−35.87	−6.44	4−3−A	−70.29	−56.15	−11.60	5−3−A	−81.29	−63.84	−9.42
4−1−B	−40.02	−30.83	−1.19	4−3−D	−67.24	−52.25	−6.08	5−3−B	−81.16	−64.09	−10.30
1−5−A	−55.32	−42.39	−3.76	5−2−A	−68.22	−54.51	−10.21	5−3−D	−79.71	−63.71	−12.19
1−5−B	−55.29	−41.59	−1.37	5−2−C	−63.14	−50.29	−7.91	5−3−G	−78.74	−60.97	−5.30
1−5−D	−53.56	−40.89	−1.61	6−1−A	−64.41	−51.12	−7.41	6−2−A	−78.64	−62.02	−8.52
2−4−A	−58.35	−45.68	−7.67	6−1−B	−62.82	−48.07	−2.08	6−2−B	−77.82	−60.91	−7.12
2−4−B	−57.84	−44.37	−4.80	1−7−A	−83.54	−62.51	−1.62	6−2−C	−77.56	−61.99	−10.33
2−4−C	−57.78	−44.13	−4.20	1−7−B	−77.03	−57.46	0.33	7−1−A	−73.88	−57.33	−4.05
3−3−A	−60.41	−48.01	−11.04	1−7−D	−75.89	−57.26	−1.12	7−1−B	−73.68	−58.43	−5.89
3−3−B	−59.04	−46.82	−9.57	1−7−J	−72.32	−55.62	−2.94	7−1−C	−73.51	−58.54	−4.94

[a] All values are in kcal/mol.

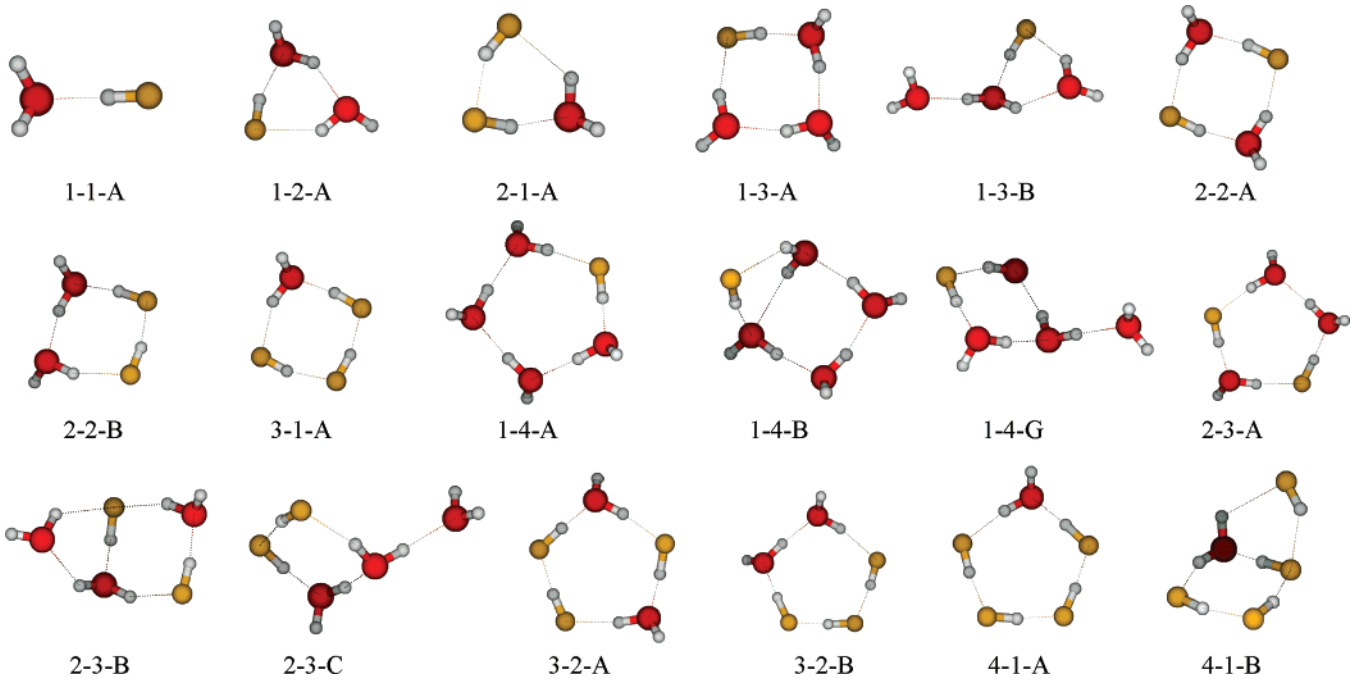

Figure 4. Representative geometries of $(HF)_m(H_2O)_n$ clusters ($m + n = 2-5$).

bond length reported for $(HF)_1(H_2O)_1$. These numbers suggest stronger H-bond interactions in trimers, but considering the non-additive, H-bond cooperative effects that are present in both HF and H_2O,any comment on the strength of the interactions based on the bond lengths in clusters of this size would be premature at this point.

3.3.3. Tetramers. $(HF)_1(H_2O)_3$. Four different geometries were optimized for this cluster. The lowest-energy structure, 1−3−A, is cyclic as shown in Figure 4. The stability of a cyclic structure has been previously reported for this system.[4,19,20] The second lowest-energy structure (1−3−B in Figure 4) has a trimer cyclic consisting in two water molecules and one HF molecule, and is less stable than the 1−3−A conformation by 5.70 kcal/mol in ΔE values and 3.30 kcal/mol in ΔG values. In 1−3−A, the H-bond distance between the fluorine and the hydrogen of the closest water molecule, R(HF···HOH), is shortened by 0.18 A and $R(H_2O\cdots HF)$ is shortened by 0.02 A, in comparison to the same values in 1−3−B.

$(HF)_2(H_2O)_2$. The lowest-energy geometry reported for this cluster, 2−2−A, is cyclic and is shown in Figure 4. This structure is in good agreement with the one reported by Chaban and co-workers.[17] The binding energy in this cluster is almost 3.5 times more than that in the $(HF)_1(H_2O)_1$ cluster, which is not surprising considering that $(HF)_2(H_2O)_2$ cluster has four

formal H-bond interactions while $(HF)_1(H_2O)_1$ cluster has just one formal H-bond interaction. For this type of cluster, a cyclic structure (2−2−B) with some H-bond interaction involving the two HF molecules is possible, as shown in Figure 4. However, the 2−2−A structure is favored by 1.01 kcal/mol in ΔE values and 0.84 kcal/mol in ΔG values. The 2−2−A structure has two shorter (and, as we will see later, stronger) hydrogen bonds of type $H_2O\cdots HF$ at 1.56 A, and two relatively longer (and, we will see later, weaker) hydrogen bonds of type $HF\cdots HOH$ at 1.71 A. The H−F bond length in this cluster is 0.956 A, which is 0.031 A longer than in the $(HF)_1(H_2O)_1$ cluster, and is 0.047 A shorter than in the $(HF)_2(H_2O)_1$ cluster. On the other hand, in 2−2−B, the $R(H_2O\cdots HF)$ distance is shorter by about 0.11 A and the $R(HF\cdots HOH)$ distance is longer by about 0.13 A in comparison with 2−2−A. The bond length of HF that is participating in the shortest H-bond interaction (the $H_2O\cdots HF$ type) is 0.034 A longer than the other one.

$(HF)_3(H_2O)_1$. Three different conformations were optimized for this cluster type. Similar to the other tetramers, the most stable structure (3−1−A) for this cluster type is also cyclic. The hydrogen bond of type $H_2O\cdots HF$remains the shortest, with almost the same H-bond length as in 2−2−B. The HF molecule participating in this $H_2O\cdots HF$interaction has the longest bond length of the three HF molecules in this cluster owing to the strength of the H-bond interaction.

3.3.4. Pentamers. $(HF)_1(H_2O)_4$. Seven different conformations were optimized for this cluster type. The cyclic structure, 1−4−A, is found to be the most stable. This structure is in good agreement with earlier reported geometries[4,20] and is favored by 2.58 kcal/mol in ΔE values when compared to the second lowest-energy structure, 1−4−B. The 1−4−B structure is in an entropically restricted bicyclic conformation, so it has a higher (i.e., less negative) ΔG value than the 1−4−G conformer.

$(HF)_2(H_2O)_3$. Of the five different conformations optimized for this cluster type, the one-ring cyclic conformation with minimal H-bond interactions between the two HF molecules, 2−3−A in Figure 4, is found to be the lowest in energy. This structure is 4.64 kcal/mol lower in energy than 2−3−B. The 2−3−B structure is a bicyclic conformation, and it has a higher free energy than 2−3−C. This relative stability trend is similar to the $(HF)_1(H_2O)_4$ cluster where the bicyclic conformation is found to be lower in energy than the conformation with a tetramer ring and another molecule H-bonded outside the ring (like in 1−4−G or 2−3−C).

$(HF)_3(H_2O)_2$. The lowest-energy structure found for this cluster is a cyclic type, 3−2−A in Figure 4. Unlike the two previous pentamer cross clusters, for this cluster type, the bicyclic or tetramer-ring conformations were not found. At the level of theory used in this study, attempts on including these kinds of structures for this cluster type resulted in cyclic structures of type 3−2−A or 3−2−B. For this cluster type, the 3−2−A conformation (pentamer ring with no H-bond interactions between the water molecules) is preferred over the 3−2−B conformation by 1.54 kcal/mol in ΔE values and 1.29 kcal/mol in ΔG values, respectively.

$(HF)_4(H_2O)_1$. Three different structures were optimized for this cluster type. The bicyclic and tetramer-ring conformations obtained for $(HF)_1(H_2O)_4$ and $(HF)_2(H_2O)_3$ clusters were observed in this cluster type as well. The most stable conformation is the cyclic structure 4−1−A, which is around 5.52 kcal/mol lower in energy than the next stable bicyclic conformation, 4−1−B. On the other hand, the third lowest-energy structure (with a tetramer ring formed by three HF molecules and one water molecule and the last HF molecule H-bonded to a hydrogen atom of the water molecule − structure not shown) is favored based on ΔG values by around 0.77 kcal/cal over the 4−1−B bicyclic conformation.

3.3.5. Hexamers. $(HF)_1(H_2O)_5$. Out of the seven optimized structures for this cluster, the cyclic structure, 1−5−A in Figure 5, is found to be the lowest in energy. Similar to the previously reported work on this cluster,[4,19] the cyclic conformation and the bicyclic conformation (1−5−B) are of similar energies. Indeed, the energy difference between 1−5−A and 1−5−B is only 0.03 kcal/mol at the mPW1B95/6-31+G(d,p) level of theory. The one-ring, cyclic conformation also has the lowest free energy value, which is 2.15 kcal/mol lower than the next lowest, 1−5−D conformation. In the 1−5−A structure, the $R(HF\cdots HOH)$ distance is reduced by 0.01 A when compared to the 1−4−A structure, and the H−F bond length is shortened by 0.0013 A. On the other hand, the $R(HF\cdots HOH)$ distance is smaller by 0.03 A, and the H−F bond length is smaller by 0.01 A, in the 1−5−B structure compared to the 1−5−A structure, an indication of slightly stronger cross interactions in this structure.

$(HF)_2(H_2O)_4$. There were six different structures optimized for this cluster, and the most stable one is a cyclic structure similar to previous clusters (2−4−A in Figure 5). The second lowest-energy structure for this cluster is multicyclic conformation similar to the 1−5−B structure. As given in Table 3, the 2−4−A structure is 0.51 kcal/mol lower in energy (which is more than in the case of the $(HF)_1(H_2O)_5$ cluster) and 2.87 kcal/mol lower in free energy than the 2−4−B structure. The third best structure based on ΔE values is shown in 2−4−C. This conformation is similar to the 2−4−B except for the changes in the orientation of HF molecules. This occurs at the expense of 0.06 kcal/mol in energy and 0.60 kcal/mol in free energy when compared to 2−4−B.

$(HF)_3(H_2O)_3$. Nine different geometries were optimized for this particular cluster, and the cyclic structure, 3−3−A, is found to be the lowest in energy. The second lowest-energy structure for this cluster is also a one-ring, cyclic structure, 3−3−B, with some H-bond interactions between the molecules of the same type. While the two structures have similar structural features, the H-bond interactions are different. The 3−3−A structure is 1.37 kcal/mol lower in energy and 1.47 kcal/mol lower in free energy than the 3−3−B structure. A bicyclic conformation was also found for this cluster, 3−3−C, but this conformation is less stable even compared to the 3−3−B structure.

$(HF)_4(H_2O)_2$. The cyclic structure (4−2−A) is found to be the lowest in energy among the four different structures optimized for this cluster. The stability of this structure is reflected in its ΔE and ΔG values, 2.37 and 4.71 kcal/mol, respectively, lower than the values for the second best conformation, the bicyclic structure 4−2−C. A bicyclic, spiro-like conformation, 4−2−D, was also optimized for this cluster type. However, this conformation is less stable even compared to the 4−2−C conformation. The spiro-like conformation is 4.42 kcal/mol higher in energy and 4.14 kcal/mol higher in free energy than the bicyclic structure 4−2−C.

$(HF)_5(H_2O)_1$: With just one H_2O molecule replacing a HF in a HF hexamer, it is not surprising that the cyclic hexamer structure 5−1−A is found to be the most stable among the four structures optimized for this cluster type. A pentamer ring formed by four HF molecules and one water molecule with one other HF molecule H-bonded to the open hydrogen atom of the water molecule (5−1−C) is also shown. Also, similar to an earlier work on the $(HF)_1(H_2O)_5$ clusters,[124] a conformation, 5−1−D, with very minimal H-bond interactions between the

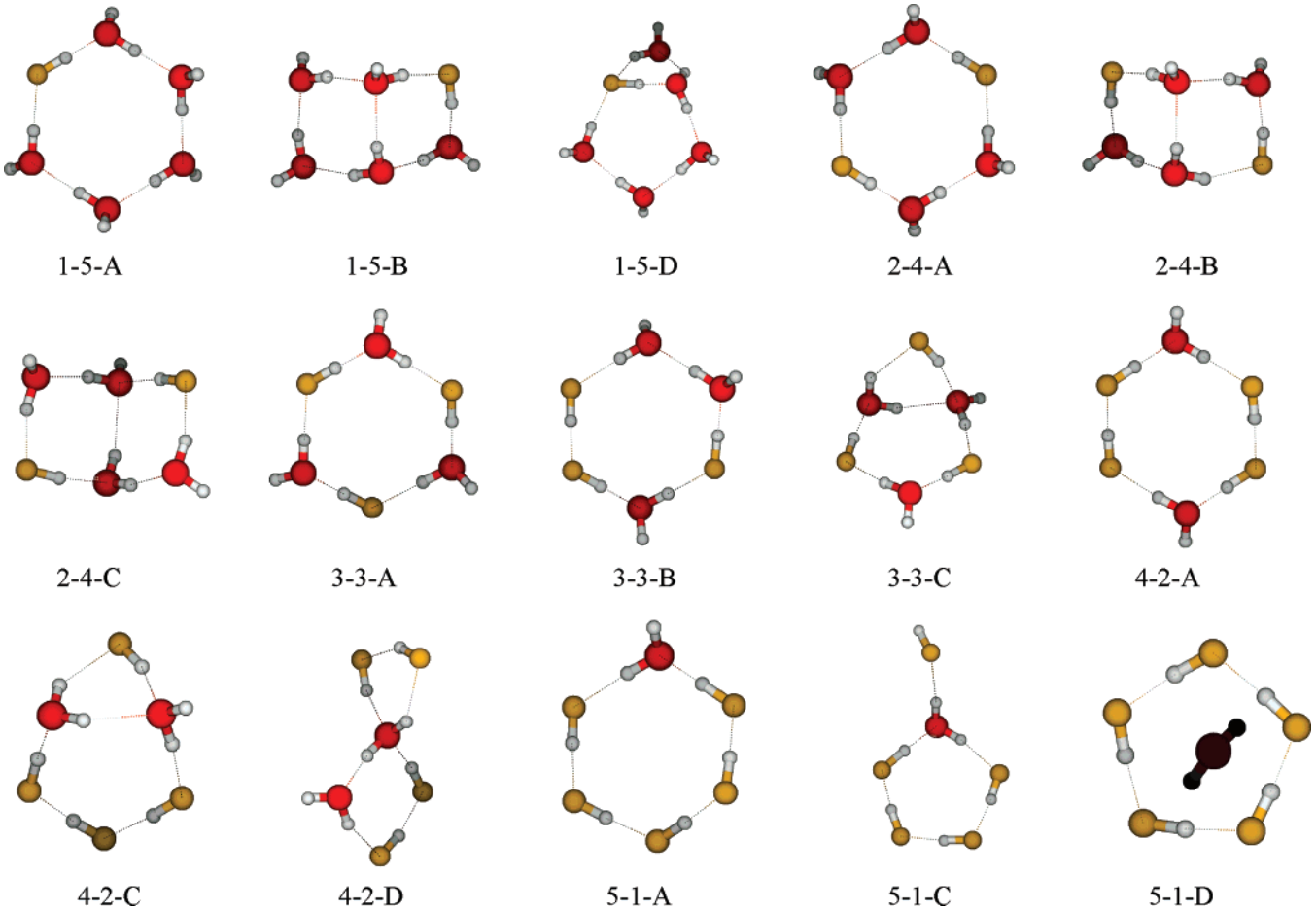

Figure 5. Representative geometries of $(HF)_m(H_2O)_n$ clusters ($m + n = 6$).

two unlike molecules was found for this cluster type but it has a much higher energy.

3.3.6. Heptamers. $(HF)_1(H_2O)_6$. Six different conformations were optimized for this cluster type, and the lowest-energy structure is the cage-like conformation 1−6−A, shown in Figure 6. The second lowest-energy structureis the bicyclic conformation 1−6−B. The 1−6−A structure is energetically preferred by 2.43 kcal/mol over the 1−6−B structure. The increase strength of the interaction between HF and H_2O molecules in 1−6−A compared to 1−6−B is reflected in the shorter $R(H_2O\cdots HF)$ distance (by 0.047 A) and the longer H−F bond length (by 0.016 A). On the other hand, the one-ring, cyclic structure 1−6−E has the lowest free energy, 1.36 and 0.71 kcal/mol lower than 1−6−A and 1−6−B, respectively.

$(HF)_2(H_2O)_5$. For this cluster type, the bicyclic conformation, 2−5−A, is found to be the lowest-energy one among six optimized structures, and the one-ring, cyclic structure, 2−5−D, is found to be the lowest free energy structure. While 2−5−A has 1.77 kcal/mol lower energy, 2−5−D has 1.38 kcal/mol lower free energy at 298 K. This cluster type also shows a spiro-like structure, 2−5−E, with two rings connected by one water molecule. The 2−5−E structure is 2.59 kcal/mol higher in energy than the 2−5−A structure and 4.35 kcal/mol higher in free energy than the 2−5−D structure.

$(HF)_3(H_2O)_4$. A multicyclic, cage-like conformation (3−4−A) is found to be the lowest energy structure out of the five different geometries optimized for this structure, but, similar to the previous heptamers, a cyclic conformation (3−4−B) is the lowest in free energy. The 3−4−A structure is 0.45 kcal/mol lower in energy but 4.69 kcal/mol higher in free energy than the 3−4−B structure. The spiro-like, bicyclic structure for this cluster type, 3−4−C, has 1.60 kcal/mol higher energy and 0.26 kcal/mol lower free energy than the 3−4−A structure.

$(HF)_4(H_2O)_3$. Out of four optimized geometries for this cluster, the lowest-energy structure (4−3−A) has more H-bond interactions between the unlike molecules and no water−water H-bond interaction. For this cluster type, an optimized cyclic conformation with one H-bond interaction between the water molecules (4−2−C) was also found (picture not shown). This structure is 1.26 kcal/mol higher in energy and 3.08 kcal/mol higher in free energy than 4−3−A. For this cluster type, the spiro-like bicyclic structure, 4−3−D, is found to be 3.05 kcal/mol higher in energy and 5.51 higher in free energy than 4−3−A.

$(HF)_5(H_2O)_2$. Five optimized geometries were considered for this cluster type. At the level of theory used in this study, this cluster combination is the smallest cluster type for which an ionized structure was identified. The lowest-energy structure is one having a bicyclic conformation and a proton transferred from fluorine to water. As mentioned earlier, we did not include the ionized structures in the analysis of our results (due to their unique character and limited number). As a result, the actual second lowest-energy structure, which is of cyclic type as well, is labeled 5−2−A. Even though the 5−2−A structure is 1.51 kcal/mol less stable than the ionized structure, it is entropically favored so its free energy is 3.02 kcal/mol lower than that of the ionized structure. The next lowest free energy structure (5−2−C) is similar to a hexamer (in terms of a ring of four HF molecules and two water molecules) but with one additional

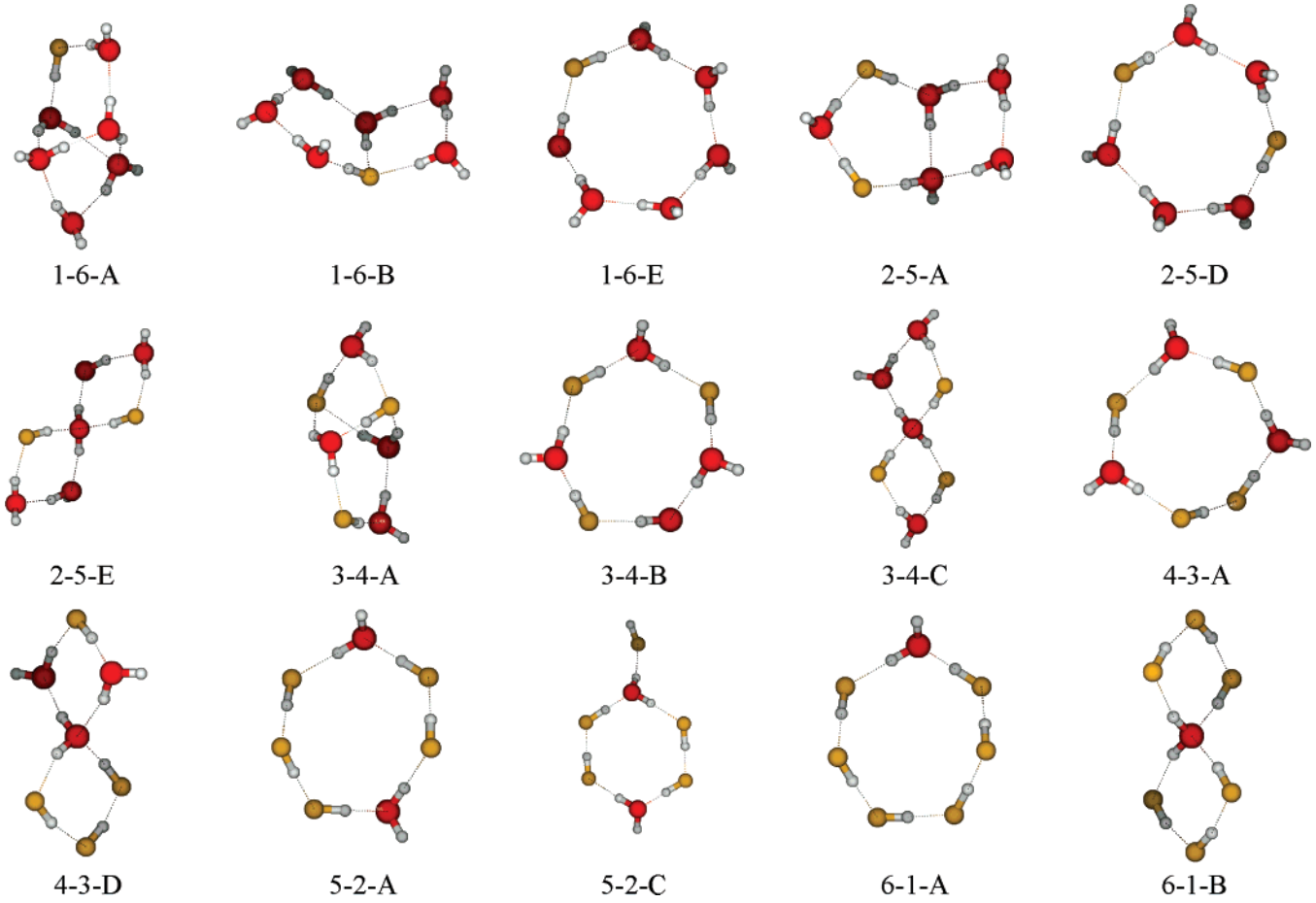

Figure 6. Representative geometries of $(HF)_m(H_2O)_n$ clusters ($m + n = 7$).

HF molecule H-bonded to one water molecule that is in the hexamer ring. The 5−2−C structure is found to be 5.08 kcal/mol higher in energy and 2.29 kcal/mol higher in free energy than 5−2−A.

$(HF)_6(H_2O)_1$. The cyclic conformation, 6−1−A, is found to be the most stable structure for this cluster type, based on both the ΔE and ΔG values. The second lowest-energy structure, 6−1−B, for this cluster mixture is the spiro-like bicyclic structure. The 6−1−A structure is 1.59 kcal/mol lower in energy and 5.32 kcal/mol lower in free energy than the 6−1−B structure. Another interesting structure (6−1−E, picture not shown), with a hexamer ring of HF molecules and one water molecule H-bonded to one HF in the ring, was also optimized. This structure is however 12.14 kcal/mol higher in energy and 8.94 kcal/mol higher in free energy than 6−1−A.

3.3.7. Octamers. $(HF)_1(H_2O)_7$. Thirteen distinct conformations were optimized for this particular cluster type. Out of these conformations, the cubic structure, 1−7−A in Figure 7, was found to be the lowest-energy one, with a ΔE value 6.50 kcal/mol lower than the next lowest-energy, multicyclic conformation, 1−7−B. On the other hand, the cyclic structure 1−7-J is entropically favored, with a free energy 1.32 kcal/mol less than the cubic structure. This class of clusters shows also few other interesting structures that are shown in Figure 7. In the cubic structure 1−7−A, the H−F bond length is elongated by 0.016 A compared to the 1−6−A structure. At this level of theory, the $R(H_2O\cdots HF)$ distance is the smallest among the $(HF)_1(H_2O)_n$ clusters, with the bond distance being reduced from 1.68 to 1.43 A as n increases from 1 to 7.

$(HF)_2(H_2O)_6$. Similar to the previous cluster type, the cubic structure, 2−6−A, is found to be the lowest-energy conformation among twelve optimized structures, 5.50 kcal/mol lower than the next lowest in energy, the multicyclic structure 2−6−B. The monocyclic structure 2−6−I is however the structure with the lowest free energy, 2.60 kcal/mol lower than 2−6−A, even though is 8.97 kcal/mol higher in energy. The structure with the second lowest free energy is the bicyclic conformation 2−6−E, 0.65 kcal/mol lower in free energy than 2−6−A. Another bicyclic structure 2−6−F, with hexamer and tetramer rings, is also optimized for this cluster type but is higher both in energy and in free energy than the bicyclic conformation with two pentamer rings (2−6−E) by 1.49 and 0.76 kcal/mol, respectively.

$(HF)_3(H_2O)_5$. Ten optimized conformations were considered for this cluster type. The lowest-energy structure is found to be the cubic structure with no H-bond interactions between HF molecules, 3−5−A in Figure 7. However, the lowest free energy structure is the cyclic structure, 3−5−G, which has a ΔG value 2.49 kcal/mol lower than 3−5−A. The second lowest-energy structure is the bicyclic structure 3−5−B, which is 3.53 kcal/mol lower in energy but 0.34 higher in free energy than the cyclic structure 3−5−G. The multicyclic conformation, 3−5−C, which was the second lowest in energy in the previous two cluster types, is found to be the third lowest in energy for this type, 1.55 and 3.93 kcal/mol higher in energy and free energy, respectively, than 3−5−B. Another interesting conformation, 3−5−D, with a spiro-like structure, is found to be 1.36 kcal/mol lower in energy than to the 3−5−G structure.

$(HF)_4(H_2O)_4$. Similar to the earlier work[17] on this cluster, the cubic structure, 4−4−A in Figure 8, is found to be the lowest energy conformation among seven optimized structures. An ionized cubic structure[17] is also identified and is found to be

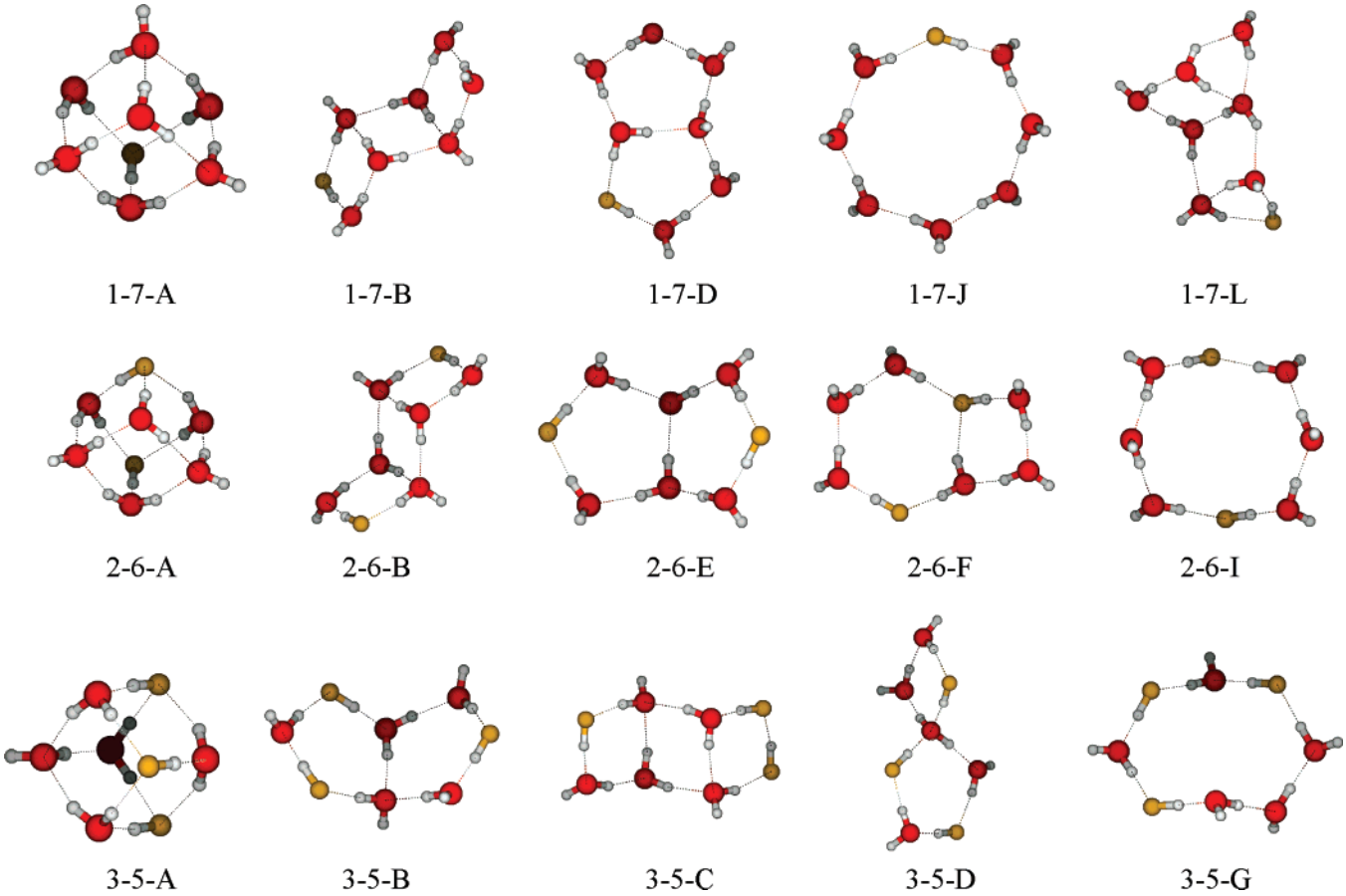

Figure 7. Representative geometries of $(HF)_m(H_2O)_n$ clusters ($m + n = 8$).

6.05 and 9.78 kcal/mol higher in energy and free energy, respectively, than 4−4−A. The second lowest-energy conformation is the multicyclic structure 4−4−B, which is however 7.02 kcal/mol higher in free energy than the lowest free energy structure 4−4−D. The spiro-like, bicyclic conformation 4−4−C and the multicyclic structure 4−4−E are also among the un-ionized structures found for this cluster type. Comparing with other $(HF)_m(H_2O)_n$ clusters with $m = n$, the average H−F bond length increases with the cluster size from 0.927 to 0.956 to 0.984 to 1.002 A as m increases from 1 to 4, indicating an increase in the cross interaction in each cluster. This is also reflected in the decrease of $R(H_2O\cdots HF)$H-bond distance, from 1.69 A in 1−1 cluster type, to an average of 1.56 A in 2−2, of 1.46 A in 3−3, and of 1.42 A in the 4−4 cluster type. This result show the same trend as reported previously by Chaban et al.[17] for 1−1, 2−2 and 4−4 clusters.

$(HF)_5(H_2O)_3$. Out of the ten un-ionized and one ionized conformations optimized for this cluster, the spiro-like, cyclic structure 5−3−A is found to be the lowest-energy one. The mono-cyclic structure, 5−3−D, is the conformation with the lowest free energy. While 5−3−D structure is 2.78 kcal/mol lower in free energy than 5−3−A, it is 1.58 kcal/mol higher in energy. Apparently, in order to form a cubic structure in an octamer cluster, it is necessary to have a minimum of four water molecules that occupies the corners of the cube. Hence, the cubic structure that was reported to be the most stable in all previous octamer clusters does not exist as the number of water molecules is less than 4. The bicyclic conformation 5−3−B is the second lowest in energy and only 1.90 kcal/mol higher in free energy than the 5−3−D structure. Another interesting structure is the multicyclic conformation 5−3−G, which is 2.55 kcal/mol higher in energy than 5−3−A and 6.89 kcal/mol higher in free energy than 5−3−D.

$(HF)_6(H_2O)_2$. For this cluster type, eight un-ionized and two ionized structures were optimized. The bicyclic conformation 6−2−A is found to be the lowest in energy, 0.82 kcal/mol lower in energy than the spiro-like conformation 6−2−B. However, the monocyclic conformation 6−2−C is entropically favored and of lowest free energy, 1.81 kcal/mol lower than the 6−2−A structure and 3.21 kcal/mol lower than the 6−2−B structure.

$(HF)_7(H_2O)_1$: Five distinct optimized conformations, including an ionized structure, were considered for this cluster type. The lowest-energy structure is the spiro-like cluster 7−1−A. The bicyclic conformation 7−1−B is just 0.20 kcal/mol higher in energy than 7−1−A, while the monocyclic conformation 7−1−C is 0.37 kcal/mol higher in energy than 7−1−A. On the other hand, 7−1−B is the lowest in free energy, 0.95 kcal/mol lower than 7−1−C and 1.84 kcal/mol lower than 7−1−A.

4. Discussion

As mentioned earlier, the principal aim of this work is to identify the possible cross-association patterns that are to be included in a bulk-phase thermodynamic model for the aqueous HF system. Recall that our goal is not to determine all possible conformations for a particular cluster type, but rather to identify the structures of greatest stability. We must note at this point that the selection of the octamer as a maximum cluster size is somewhat arbitrary, though previous work on this system (either in a mixture or as pure components) would support this choice as rationale.[10,18,26,48,51,53,66,100,113] Accordingly, we assume that the presence of larger clusters will not change significantly the results in the present analysis. More importantly, we assume

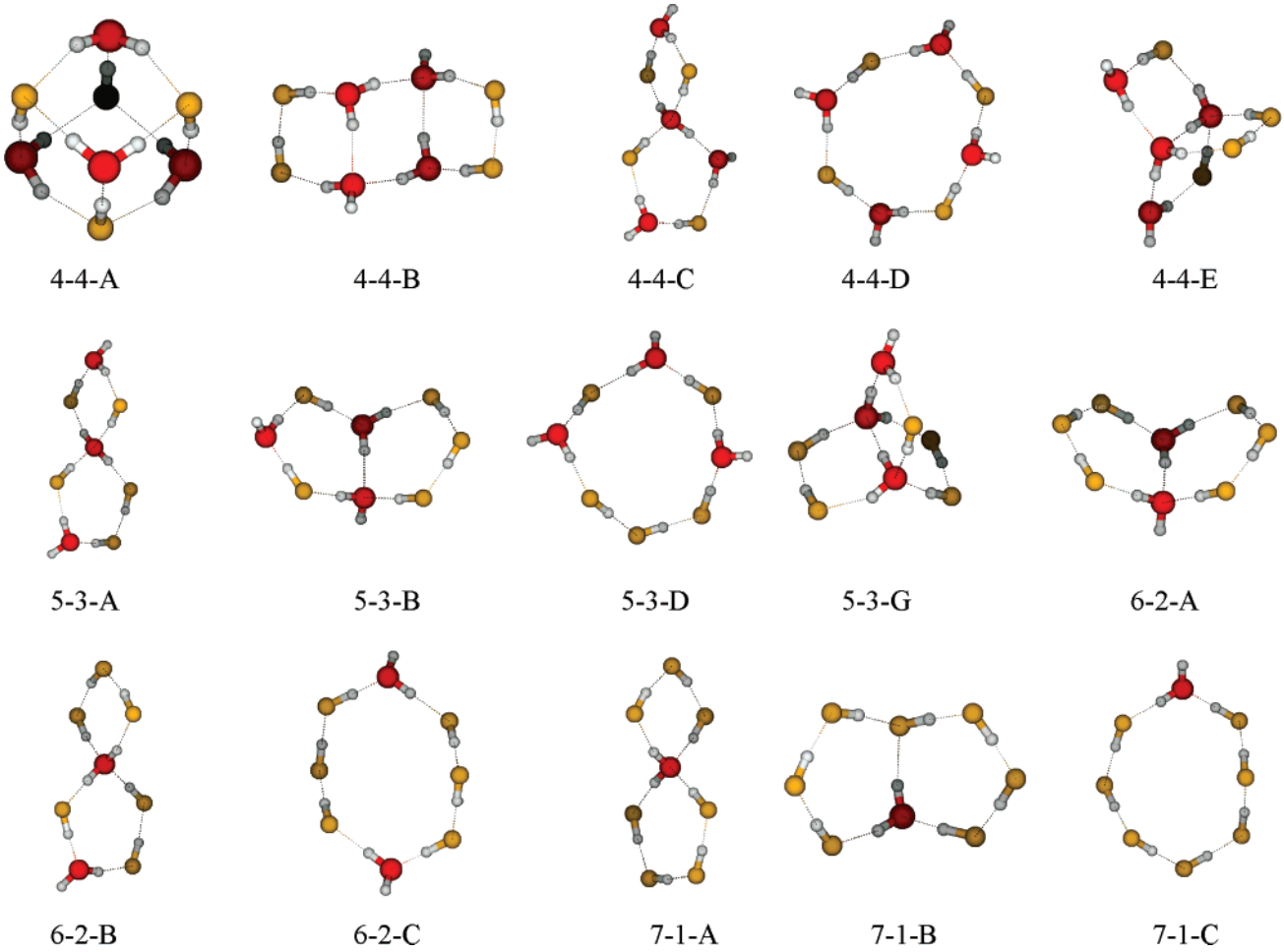

Figure 8. Representative geometries of $(HF)_m(H_2O)_n$ clusters ($m + n = 8$).

that the most stable conformations for each cluster type are identified, and that any cluster size and conformations that were not considered would not modify our findings considerably. The results in this study are dependent on other factors and approximations (i.e., the choice of level of theory used, the accuracy of the calculated frequencies used in determining ΔG_{298}, the non-inclusion of the basis set superposition error, the absence of solvent effects, etc), and the inclusion of any of these will likely increase the accuracy of our results. We assumed, however, that none of these factors would substantially change the main findings (i.e., the relative stabilities of various clusters and the properties derived from these) of the study.

Also, anharmonicity effects on the calculated vibrational frequencies have been studied on clusters similar to the one investigated in the present study by several groups.[17,125,126] The goal of these studies was mainly on including the anharmonic effects with the purpose of assigning experimentally determined frequencies. These studies showed that including anharmonicity can both increase and decrease the calculated values of low-energy vibrational frequencies (Gibbs energy values are most sensitive to these vibrational frequencies). Predicting the changes in Gibbs energy values on the inclusion of anharmonicity effects is therefore unreliable and will not be done here. One would expect though that anharmonicity effects will reduce the vibrational frequencies, increase the number of available states and therefore lower the Gibbs free energy.

4.1. Average Hydrogen−Bond Strengths. As an initial analysis of our work, we used the structural and energetic information obtained for various optimized clusters in this study to investigate the average strength for the different types of hydrogen bonds in this mixture. In an un-ionized cross-association cluster, there are four potential types of H-bond interactions: the $H_2O\cdots H-F$ type denoted O···HF, the $H_2O\cdots H-OH$ type denoted O···HO, the $HF\cdots H-F$ type denoted F···HF, and the $HF\cdots H-OH$ type denoted F···HO. For each un-ionized conformation considered, we determined the number of H-bond interactions and classified them based on these four types. Since the internuclear distances can vary significantly with the cluster size and for various conformations, identifying the number of hydrogen bonds cannot be done easily by visually inspecting the structure. Accordingly, we count the number of interatomic distances involving a hydrogen atom and either a fluorine or an oxygen atom that are between 1.1 and 2.2 A. We chose this range after examining histograms of all atomic distances to separate out the chemical bonds (at distances lower than 1.1 A) as well as the non-H-bonded, dispersive interactions (at distances greater than 2.2 A). In doing this, we found that, for example, in the 4−4−A structure, there are four O···HF hydrogen bonds, eight F···HO hydrogen bonds, and no O···HO or F···HF hydrogen bonds. A similar analysis was performed for all un-ionized structures (including pure clusters) optimized in this work. The ionized structures were not included during the regression. There are two reasons for this: (i) some of the H-bond interactions appearing in these ionized clusters are different than those appearing in the un-ionized clusters, and (ii) the number of ionized clusters found is not large enough to allow an analysis of these distinct types of H-bond interactions.

TABLE 4: Average Energies, Enthalpies at 0 K, and Free Energies at 298 K (in kcal/mol) for Various Types of H−Bond Interactions as Well as R^2 Values for the Multiple Linear Regressions

	regression coefficients					
	all structures (224)			most stable structures (42)		
interaction type	ΔE	ΔH_0	ΔG	ΔE	ΔH_0	ΔG
$H_2O\cdots H-F$	−15.01	−11.97	−2.74	−17.35	−13.74	−2.81
$H_2O\cdots H-OH$	−6.74	−4.91	0.50	−6.85	−5.22	0.19
$HF\cdots H-F$	−8.38	−6.59	−0.46	−8.26	−6.55	−0.49
$HF\cdots H-OH$	−3.94	−3.01	0.21	−2.26	−1.72	−0.81
R^2	0.9906	0.9887	0.7509	0.9945	0.9927	0.9521

Once the H-bond interactions were counted and classified for all un-ionized clusters, a multiple linear regression was performed according to

$$Z = Z^{O\cdots HF}\cdot n^{O\cdots HF} + Z^{O\cdots HO}\cdot n^{O\cdots HO} + Z^{F\cdots HF}\cdot n^{F\cdots HF} + Z^{F\cdots HO}\cdot n^{F\cdots HO} \quad (2)$$

where Z is ΔE, ΔH_0, or ΔG and $n^{X\cdots HY}$ are the number of hydrogen bonds of $X\cdots HY$ type in each cluster. By doing this analysis, it is assumed that the interaction energy in a cluster is only due to the H-bond interactions.

The average H-bond strength and the corresponding regression R^2 values for the three energetic parameters associated with eq 2 are listed in Table 4. As one can see, based on the R^2 values, the fits are reasonable, and the results of all three regressions indicate that the strongest H-bond interaction is the $H_2O\cdots H-F$ type while the weakest is the $HF\cdots H-OH$ type. We carried out linear regressions based on eq 2 but including only subsets of all optimized structures. We found (although we did not include the results) that the relative strength of H-bond interaction remains the same if the regression is done on subsets that include only clusters of the same size.

Since including all structures in the regression analysis also includes the structures that are least favorable energetically, the average H-bond strength analysis was also performed by including only the most stable structures for each cluster type. The average H-bond strength and the corresponding regression R^2 values for the three energetic parameters, with only the 42 (14 pure clusters and 28 cross clusters) structures (the ones of lowest ΔE, ΔH_0, or ΔG values, respectively, for each cluster type) are also listed in Table 4. The results of all three regressions indicate that the strongest H-bond interaction is still the $H_2O\cdots H-F$ type. Also, similar to the regression results with all the structures, based on ΔE and ΔH_0 values, the weakest H-bond interaction is the $HF\cdots H-OH$ type, while based on ΔG values, the $H_2O\cdots H-OH$ type is the weakest. Based on the calculated H-bond strengths for smaller clusters, where experimental data is available, the level of theory used here, mPW1B95/6-31+G(d,p), seems to overestimate slightly the strength of the H-bond interactions. Assuming that the same trend is true for larger clusters as well, the average values reported in this section may be slightly overestimated. The relative strength among various types of H-bond interactions is expected, however, to be correctly characterized.

4.2. Distribution of Mixed Clusters. With both HF and H_2O showing several association patterns in pure and mixture compositions, it is relevant to study the distribution of these association schemes as a function of composition. Note that the composition of a cluster is defined here as the mole fraction of HF in the $(HF)_m(H_2O)_n$ cluster, which is $x_{HF} = m/(m+n)$. For example, the composition of the $(HF)_2(H_2O)_3$ cluster is $x_{HF} = 0.40$.

A first step in analyzing the data is to represent the binding energies defined for eq 1 as a function of composition. Panels a and b of Figure 9 show the minimum values of ΔE and ΔG, respectively, for various compositions of the mixture. (The plot based on ΔH_0 values is similar to the one based on ΔE, so it is not shown or discussed.) Since we obtained several conformations for each cluster type, the plots show only the structures of lowest energy or lowest free energy, respectively. Both these plots indicate that for clusters containing the same number of molecules (which are connected by lines for guidance), the most stable $(HF)_m(H_2O)_n$ clusters are the ones closest to equimolar. For clusters containing an even number of molecules, the highest binding energies are obtained when $m = n$.

While an analysis based on the representations in Figure 9 includes the various compositions associated with the clusters, it does not allow a direct comparison between clusters of different sizes. Here again, the size of a cluster is defined as the total number of molecules in the cluster, that is $m + n$. It is therefore preferred to define a "normalized" formation process, which is the process of forming a part of a cluster that contains only one mole/molecule (or forming a part of a cluster from one mol/molecule of constituents):

$$\frac{m}{m+n}\,HF + \frac{n}{m+n}\,H_2O \rightarrow \frac{1}{m+n}\,(HF)_m(H_2O)_n \quad (3)$$

The zero-point exclusive energy and the Gibbs free energy at 298.15 K for this process are labeled $\Delta\bar{E}$ and $\Delta\bar{G}_{298}$ (or $\Delta\bar{G}$ for simplicity), respectively. These values are related to the ΔE and ΔG through

$$\Delta\bar{E} = \Delta E/(m+n) \quad (4)$$

and

$$\Delta\bar{G} = \Delta G/(m+n) \quad (5)$$

Using these normalized values of the binding energy allows for a more direct comparison between the results obtained for cluster of different sizes.

Figure 10a,b shows $\Delta\bar{E}$ and $\Delta\bar{G}$ as a function of the cluster composition. Since, $\Delta\bar{E}$ and $\Delta\bar{G}$ are obtained by dividing ΔE and ΔG by $m + n$ (i.e., the size of the cluster), the shape of the lines connecting the clusters of the same size do not change, and still show preference for equimolar structures. Comparing clusters of different sizes, the graph for electronic energies shows preference for larger clusters versus that of smaller-size clusters. Across the whole range of compositions, the octamers are the preferred cluster type, with some heptamers, hexamers and pentamers of similar binding energies at higher HF concentrations. On the other hand, the free energy $\Delta\bar{G}$ values (which is the determining factor in the cluster stability) show preference for the hexamer, with some heptamers, pentamers and octamers favored at lower HF concentrations, and relatively more pentamers and heptamers than octamers at higher HF concentrations. In both cases, smaller size clusters do not seem to be preferred.

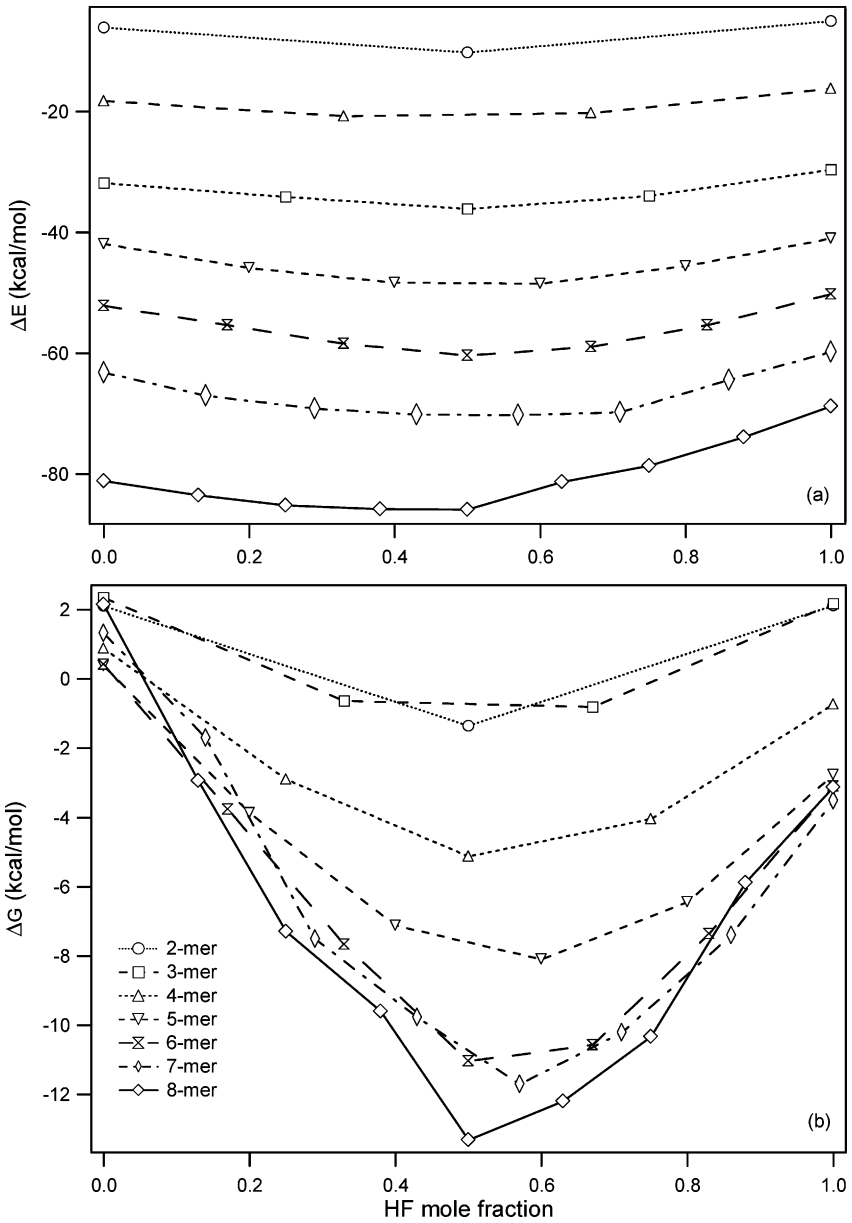

Figure 9. ΔE and ΔG vs the cluster composition.

The graphs in Figure 10 include information about both the size and the composition of a certain cluster and are more suitable to directly compare relative stabilities for various clusters. Because the clusters are used to model a solution of a certain concentration, the comparison is still, however, limited to clusters or combinations of clusters that have the same composition. The first step in determining the preferred clusters in a HF−H_2O mixture is to choose a mole fraction, which is named the "target" mole fraction and is labeled x_{target}. Once the target mole fraction is chosen, the clusters are divided in three classes. One class, called class I, contains clusters with compositions smaller than the target ($x_{HF} < x_{target}$), one other class, called class II, contains clusters with compositions larger than the target ($x_{HF} > x_{target}$), and the last class, called class III, contains any cluster with the same composition as the target ($x_{HF} = x_{target}$). Actually, class III contains none or a very small number of clusters. In our study, with the exception of $x_{target} = 0.00$ or $x_{target} = 1.00$, the most number of members in class III is obtained for $x_{target} = 0.50$, for which there are four members in this class: $(HF)_1(H_2O)_1$, $(HF)_2(H_2O)_2$, $(HF)_3(H_2O)_3$, and $(HF)_4(H_2O)_4$. Other distinctive cases are those in which x_{target} is 0.33 or 0.67, when class III contains two members: $(HF)_1(H_2O)_2$ and $(HF)_2(H_2O)_4$ or $(HF)_2(H_2O)_1$ and $(HF)_4(H_2O)_2$, respectively. In all other cases, class III will contain only one or no members. The number of clusters in classes I and II is the difference between the total number of cluster types considered (42) and the number of clusters in class III.

Modeling a mixture with the x_{target} composition can be done by considering only the cluster (or clusters) from class III, or by combinations of clusters from classes I and II, with the condition that at least one cluster from each class I and class II are included. This latter case is similar to mixing two solutions on different concentrations when only concentrations between the two original ones can be obtained. We will discuss in more detail only the case in which one cluster from each class I and class II are considered, but extensions for combinations of more than two clusters can be made based on this case (by combining two clusters first and further combining this combination of two clusters to the third cluster). Let us denote the composition of the class I cluster, $(HF)_{m_I}(H_2O)_{n_I}$, by x_I and its normalized binding energy by $\Delta\bar{E}_I$, and the composition of the class II cluster, $(HF)_{m_{II}}(H_2O)_{n_{II}}$, by x_{II} and its normalized binding energy

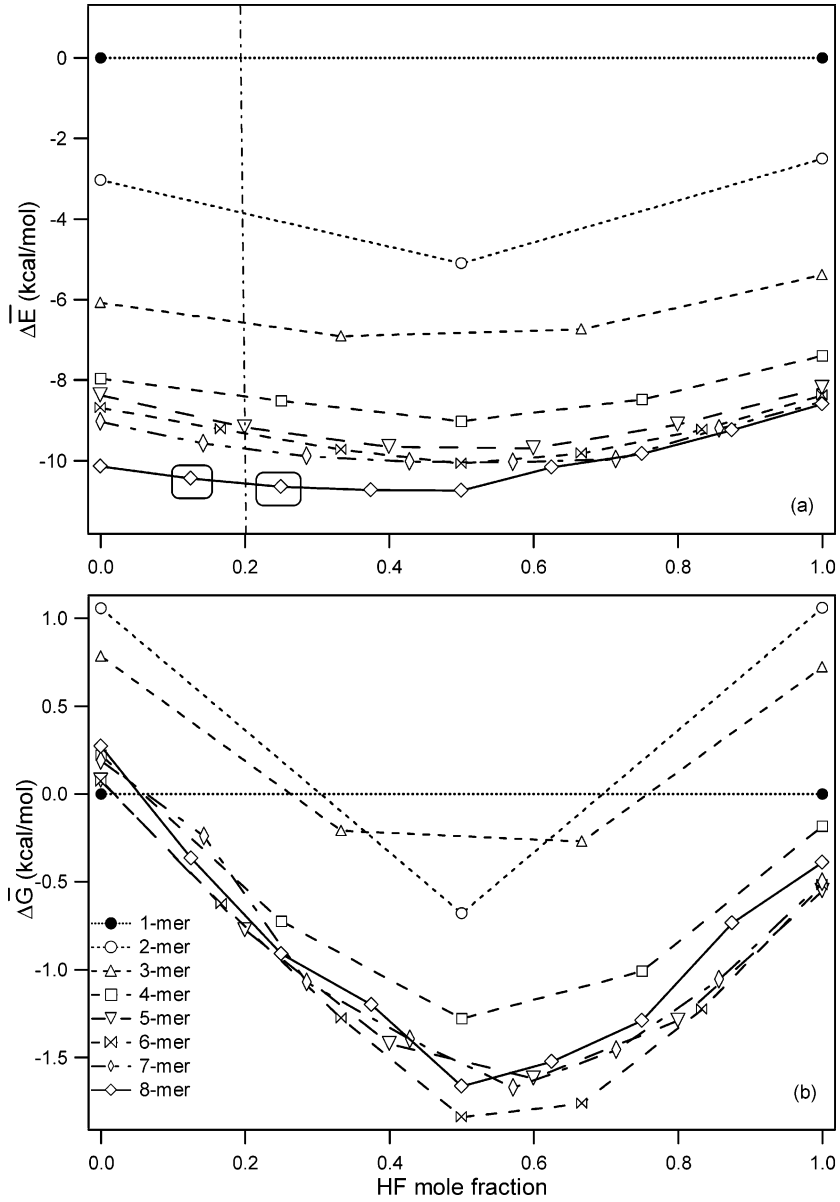

Figure 10. Normalized $\Delta\bar{E}$ and $\Delta\bar{G}$ vs the cluster composition.

by $\Delta\bar{E}_{II}$. The binding energy obtained for a combination of two clusters at a certain composition x_{target} is given by

$$\Delta\bar{E}_{I-II} = \frac{x_{target} - x_I}{x_{II} - x_I}\Delta\bar{E}_{II} + \frac{x_{II} - x_{target}}{x_{II} - x_I}\Delta\bar{E}_I \qquad (6)$$

This is the energy associated with the process of making a (100·x_{target})% mixture containing only one mol/molecule (similar to the process in eq 3), as a combination of $(HF)_{m_I}(H_2O)_{n_I}$ and $(HF)_{m_{II}}(H_2O)_{n_{II}}$ clusters:

$$x_{target}HF + (1 - x_{target})H_2O \rightarrow \frac{1}{m_I + n_I}\frac{x_{II} - x_{target}}{x_{II} - x_I}(HF)_{mI}$$
$$(H_2O)_{nI} + \frac{1}{m_{II} + n_{II}}\frac{x_{target} - x_I}{x_{II} - x_I}(HF)_{mII}(H_2O)_{nII} \quad (7)$$

The $\Delta\bar{E}$ value given in eq 6 can be obtained graphically at the intersection of the line connecting the two clusters, the (x_I, $\Delta\bar{E}_I$) point and the (x_{II}, $\Delta\bar{E}_{II}$) point, respectively, in the representation shown in Figure 10a with a vertical line at the x_{target} composition. A similar expression to the one in eq 6 can be written, and the same graphical exercise can be done for $\Delta\bar{G}$.

To demonstrate this approach, we choose a target HF mole fraction of 20%. Only one cluster, $(HF)_1(H_2O)_4$, from the ones considered in this work has the same composition as the target mole fraction, so class III contains only one member. We can create an HF−H_2O mixture considering only this cluster type or by any composition of clusters with smaller and with larger compositions. In this example, we choose the $(HF)_1(H_2O)_7$ cluster (as the member of class I) and the $(HF)_2(H_2O)_6$ cluster (as the member of class II). The composition of the $(HF)_1(H_2O)_7$ cluster is $x_I = 0.125$, and the composition of the $(HF)_2(H_2O)_6$ cluster is $x_{II} = 0.25$. The normalized binding energy for making clusters that contains only one molecule (eq 7), with a composition of $x_{target} = 0.20$, from combinations of $(HF)_1(H_2O)_7$ and $(HF)_2(H_2O)_6$ clusters, is given by

$$\Delta\bar{E}_{17-26} = \frac{0.200 - 0.125}{0.250 - 0.125}(-10.65) + \frac{0.250 - 0.200}{0.250 - 0.125}(-10.44) = -10.57 \text{ kcal/mol} \quad (8)$$

TABLE 5: The Top Three Cross−Cluster Combinations That Are Likely to Be Present Across x_{HF}, Based on $\Delta\bar{E}$ and $\Delta\bar{G}$ Values (in kcal/mol)

x_{HF}	lowest $\Delta\bar{E}$ cross associates	$\Delta\bar{E}$	lowest $\Delta\bar{G}$ cross associates	$\Delta\bar{G}$
0.0	$(HF)_0-(H_2O)_8$	−10.14	$(HF)_0-(H_2O)_1$	0.00
	$(HF)_0-(H_2O)_8 + (HF)_0-(H_2O)_7$	−9.59	$(HF)_0-(H_2O)_8 + (HF)_0-(H_2O)_6$	0.04
	$(HF)_0-(H_2O)_8 + (HF)_0-(H_2O)_6$	−9.42	$(HF)_0-(H_2O)_8 + (HF)_0-(H_2O)_5$	0.04
0.1	$(HF)_0-(H_2O)_8 + (HF)_1-(H_2O)_7$	−10.38	$(HF)_0-(H_2O)_1 + (HF)_1-(H_2O)_4$	−0.39
	$(HF)_0-(H_2O)_8 + (HF)_2-(H_2O)_6$	−10.35	$(HF)_0-(H_2O)_1 + (HF)_2-(H_2O)_4$	−0.38
	$(HF)_0-(H_2O)_8 + (HF)_3-(H_2O)_5$	−10.30	$(HF)_0-(H_2O)_1 + (HF)_1-(H_2O)_5$	−0.38
0.2	$(HF)_1-(H_2O)_7 + (HF)_2-(H_2O)_6$	−10.57	$(HF)_1-(H_2O)_4$	−0.78
	$(HF)_0-(H_2O)_8 + (HF)_2-(H_2O)_6$	−10.55	$(HF)_0-(H_2O)_1 + (HF)_2-(H_2O)_4$	−0.77
	$(HF)_1-(H_2O)_7 + (HF)_3-(H_2O)_5$	−10.53	$(HF)_1-(H_2O)_5 + (HF)_2-(H_2O)_4$	−0.76
0.3	$(HF)_2-(H_2O)_6 + (HF)_3-(H_2O)_5$	−10.68	$(HF)_1-(H_2O)_4 + (HF)_2-(H_2O)_4$	−1.15
	$(HF)_2-(H_2O)_6 + (HF)_4-(H_2O)_4$	−10.67	$(HF)_0-(H_2O)_1 + (HF)_2-(H_2O)_4$	−1.15
	$(HF)_1-(H_2O)_7 + (HF)_3-(H_2O)_5$	−10.64	$(HF)_1-(H_2O)_5 + (HF)_2-(H_2O)_4$	−1.15
0.4	$(HF)_3-(H_2O)_5 + (HF)_4-(H_2O)_4$	−10.73	$(HF)_2-(H_2O)_4 + (HF)_3-(H_2O)_3$	−1.50
	$(HF)_2-(H_2O)_6 + (HF)_4-(H_2O)_4$	−10.70	$(HF)_1-(H_2O)_4 + (HF)_3-(H_2O)_3$	−1.49
	$(HF)_3-(H_2O)_5 + (HF)_5-(H_2O)_2$	−10.67	$(HF)_2-(H_2O)_5 + (HF)_3-(H_2O)_3$	−1.48
0.5	$(HF)_4-(H_2O)_4$	−10.74	$(HF)_3-(H_2O)_3$	−1.84
	$(HF)_3-(H_2O)_5 + (HF)_5-(H_2O)_2$	−10.45	$(HF)_3-(H_2O)_3 + (HF)_4-(H_2O)_4$	−1.75
	$(HF)_3-(H_2O)_5 + (HF)_5-(H_2O)_3$	−10.44	$(HF)_4-(H_2O)_4$	−1.66
0.6	$(HF)_4-(H_2O)_4 + (HF)_5-(H_2O)_2$	−10.37	$(HF)_3-(H_2O)_3 + (HF)_4-(H_2O)_2$	−1.79
	$(HF)_4-(H_2O)_4 + (HF)_6-(H_2O)_2$	−10.37	$(HF)_4-(H_2O)_4 + (HF)_4-(H_2O)_2$	−1.72
	$(HF)_4-(H_2O)_4 + (HF)_7-(H_2O)_1$	−10.34	$(HF)_4-(H_2O)_3 + (HF)_4-(H_2O)_2$	−1.70
0.7	$(HF)_4-(H_2O)_4 + (HF)_5-(H_2O)_2$	−10.01	$(HF)_4-(H_2O)_2 + (HF)_5-(H_2O)_1$	−1.66
	$(HF)_4-(H_2O)_4 + (HF)_6-(H_2O)_2$	−10.01	$(HF)_4-(H_2O)_2 + (HF)_4-(H_2O)_1$	−1.64
	$(HF)_3-(H_2O)_5 + (HF)_5-(H_2O)_2$	−9.99	$(HF)_4-(H_2O)_2 + (HF)_5-(H_2O)_0$	−1.64
0.8	$(HF)_6-(H_2O)_2 + (HF)_7-(H_2O)_1$	−9.59	$(HF)_4-(H_2O)_2 + (HF)_5-(H_2O)_1$	−1.33
	$(HF)_6-(H_2O)_2 + (HF)_8-(H_2O)_0$	−9.58	$(HF)_5-(H_2O)_2 + (HF)_5-(H_2O)_1$	−1.29
	$(HF)_5-(H_2O)_2 + (HF)_7-(H_2O)_1$	−9.57	$(HF)_4-(H_2O)_1 + (HF)_4-(H_2O)_1$	−1.29
0.9	$(HF)_7-(H_2O)_1 + (HF)_8-(H_2O)_0$	−9.11	$(HF)_5-(H_2O)_1 + (HF)_5-(H_2O)_0$	−0.96
	$(HF)_7-(H_2O)_1 + (HF)_7-(H_2O)_0$	−9.10	$(HF)_5-(H_2O)_1 + (HF)_6-(H_2O)_0$	−0.95
	$(HF)_6-(H_2O)_2 + (HF)_8-(H_2O)_0$	−9.09	$(HF)_5-(H_2O)_1 + (HF)_7-(H_2O)_0$	−0.94
1.0	$(HF)_8-(H_2O)_0$	−8.60	$(HF)_5-(H_2O)_0$	−0.55
	$(HF)_7-(H_2O)_0 + (HF)_8-(H_2O)_0$	−8.57	$(HF)_5-(H_2O)_0 + (HF)_6-(H_2O)_0$	−0.53
	$(HF)_7-(H_2O)_0 + (HF)_7-(H_2O)_0$	−8.54	$(HF)_5-(H_2O)_0 + (HF)_7-(H_2O)_0$	−0.53

which is lower than the $\Delta\bar{E}$ value for $(HF)_1(H_2O)_4$ cluster (−9.17 kcal/mol). The result shows that a 20% HF mixture is energetically preferred to be formed from the combination of the $(HF)_1(H_2O)_7$ and $(HF)_2(H_2O)_6$ clusters rather than from exclusively $(HF)_1(H_2O)_4$ clusters. Actually, the combination of the $(HF)_1(H_2O)_7$ and $(HF)_2(H_2O)_6$ clusters is the energetically most favorable combination for a 20% HF mixture, as listed in Table 5. This example is also shown graphically in Figure 10a in which the $(HF)_1(H_2O)_7$ and $(HF)_2(H_2O)_6$ clusters are boxed.

If one wants to model an HF−water mixture with the particular compositions of 0.33, 0.50, or 0.66, the compositions for which class III contains two or more clusters, any combinations of these clusters will have the same composition as the mixture. In this case, for a combination of n_{III-a} clusters with n_{III-b} clusters of class III, the binding energy obtained for the cluster combination is

$$\Delta\bar{E}_{III-III} = \frac{n_{III-a}}{n_{III-a} + n_{III-b}}\Delta\bar{E}_{III-a} + \frac{n_{III-b}}{n_{III-a} + n_{III-b}}\Delta\bar{E}_{III-b} \quad (9)$$

In summary, for modeling HF−water mixtures with any concentration using cluster calculations, one needs to do so by using clusters (or combinations of clusters) with the same composition (i.e., class III clusters) or combinations of clusters with higher and lower compositions (one or more clusters from class I and one or more clusters from class II). The combinations of greater stability (i.e., of lower energy or of lower free energy) are obtained from clusters with the lowest (i.e., more negative) $\Delta\bar{E}$ and $\Delta\bar{G}$ values. These key clusters (of lowest energy or of lowest free energy) change with the composition, and are shown in Figures 11 and 12 by filled squares connected by dashed lines. All other clusters (by themselves or in combinations) will not give the most favorable combinations but might provide combinations that are of similar energy or free energy to the most favorable ones. Table 5 lists the top three options, based on $\Delta\bar{E}$ and $\Delta\bar{G}$ values, as a function of the HF composition in the mixture. As one can see, there are very small energy differences between these options, so the likelihood for the second and third options to be present at a respective composition is almost the same as the best option.

The two graphs in Figures 11 and 12 illustrate the distribution of the key cross clusters and their most stable binary combinations across the HF composition, based on $\Delta\bar{E}$ and $\Delta\bar{G}$ values, respectively. These plots show also the most stable pure cross clusters (i.e., without combining with any other cluster type) at the respective mole fractions. Here, the filled squares that are connected through dashed lines indicate the most stable clusters either by themselves or as combinations of them. The empty squares indicate the clusters that are the most stable at their respective mole fraction but are not preferred over the combinations of clusters that are indicated by filled boxes. For example, at $x_{HF} = 0.40$, the pure $(HF)_2(H_2O)_3$ ($\Delta\bar{E} = -9.66$ kcal/mol) will have a lower $\Delta\bar{E}$ value than the combination of $(HF)_1(H_2O)_4$ and $(HF)_3(H_2O)_2$ clusters ($\Delta\bar{E}_{I-II} = -9.42$ kcal/mol), for which the $\Delta\bar{E}$ value is given by eq 6 or by the value at $x_{HF} = 0.40$ of the line connecting the two clusters in Figure 10a or Figure 11. However, at $x_{HF} = 0.40$, the pure $(HF)_2(H_2O)_3$ will have a higher $\Delta\bar{E}$ value than many other cluster combinations, such as $(HF)_2(H_2O)_4$ with $(HF)_4(H_2O)_3$ for which $\Delta\bar{E}_{I-II} = -9.81$ kcal/mol or $(HF)_1(H_2O)_6$ with $(HF)_5(H_2O)_3$ for which $\Delta\bar{E}_{I-II} = -9.89$ kcal/mol. Note that the combination of lowest energy for $x_{HF} = 0.40$, as seen in Figure 11 and determined based on the data in Table 5, is the combination of $(HF)_3(H_2O)_5$ with $(HF)_4(H_2O)_4$ for which $\Delta\bar{E}_{I-II} = -10.73$ kcal/mol.

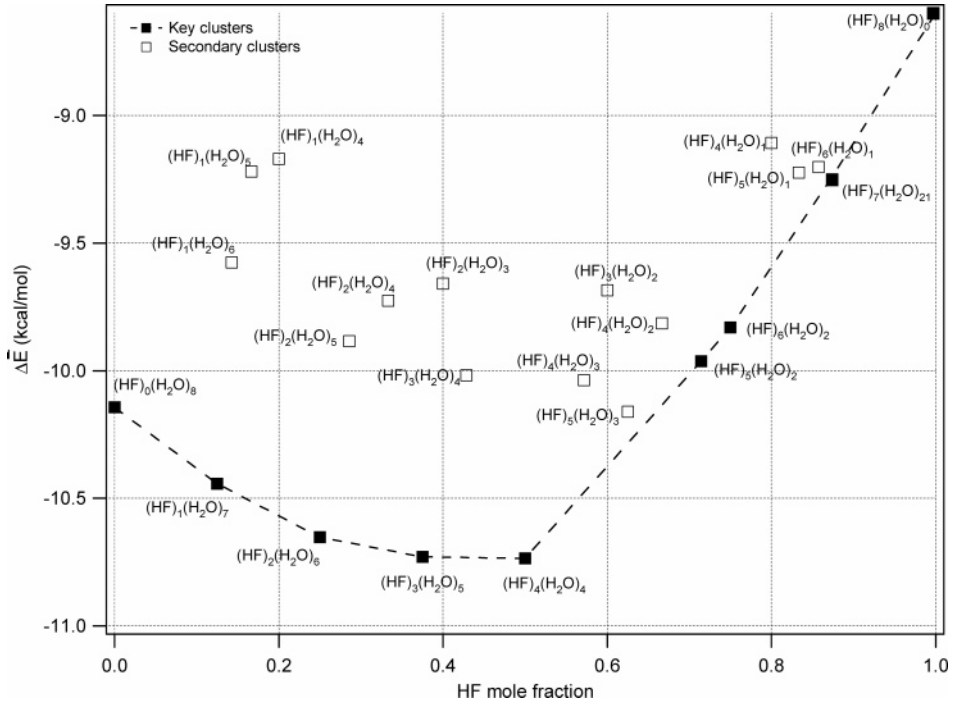

Figure 11. The preferred cluster combinations vs the cluster composition based on $\Delta\bar{E}$ values.

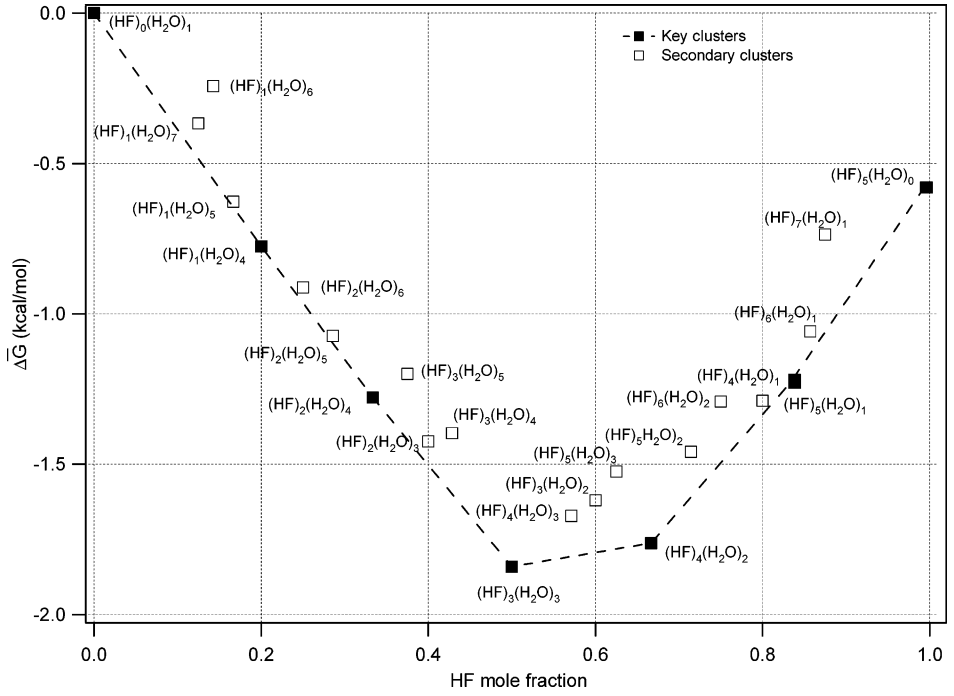

Figure 12. The preferred cluster combinations vs the cluster composition based on $\Delta\bar{G}$ values.

5. Conclusion

To our knowledge, there is no comprehensive study in the literature reporting the self-as well as cross-association patterns for HF−H_2O mixture using computations on clusters as high eight molecules in size. In the present study, the structures and energetics of all 214 different conformations of $(HF)_m(H_2O)_n$ clusters with $m + n = 2-8$ were obtained at the mPW1B95/6-31+G(d,p) level of theory. The primary objective of this work is to extract the cross-cluster information that will be applied in the development of a bulk-phase thermodynamic model for this particular mixture. In that aspect, the results are focused on the association patterns in this mixture rather than on the ionization of HF and the proton-transfer process, even though, at this level of theory, six different ionized conformations were also identified. However, with the exception of the $(HF)_5(H_2O)_2$ cluster, the un-ionized clusters are found to be more stable than the ionized ones.

The values of the energy and the free energy of formation for various cluster types indicate that the combinations with same or similar number of HF and H_2O molecules are the most stable. While the energy values suggest the formation of complex networks such as cubic and cage-like structures for larger clusters, the free energy values indicate the monocyclic structures to be the most stable. Typically, a structure that forms

a more complex H-bond network characterized by a lower energy does have low entropy, and this is reflected in higher free energy values.

We analyzed the strength of the H-bond interactions using multiple linear regressions. All three regressions, based on ΔE, ΔH_0, and ΔG_{298}, indicate that $H_2O\cdots HF$ interaction is the strongest of the four different H-bond interactions that could occur in an un-ionized cluster. The $H_2O\cdots HF$ H-bond interaction being the strongest is also consistent with the ionization of HF and formation of H_3O^+ and F^- ions, which was obtained in some clusters. The strength of this particular H-bond interaction is also reflected in the geometrical parameters (i.e., longer H−F bond length and shorter $H_2O\cdots HF$ bond distance) especially for the larger clusters.

Finally, an analysis was performed to provide those cross associates that were most likely to be present at various compositions in this mixture. It is this knowledge that can be directly incorporated into a bulk-phase thermodynamic model. Future work will look to include this information in the development of a robust and predictive equation of state for the aqueous hydrogen fluoride system.

Acknowledgment. This work was partially supported by the American Chemical Society, Petroleum Research Fund (PRF42227−AC9) and the Center for Manufacturing Research, Tennessee Technological University. We would also like to acknowledge Mike Renfro for computational assistance and the Computer Aided Engineering Laboratory at Tennessee Technological University for providing the computational facilities for this work. Also, we would like to acknowledge Dr. Chaban and Dr. Burda for providing supplemental information on their optimized cluster geometries.

Supporting Information Available: The Supporting Information contains the Cartesian coordinates and figures for all optimized structures in this work. This material is available free of charge via the Internet at http://pubs.acs.org.

References and Notes

(1) Munter, P. A.; Aepli, O. T.; Kossatz, R. A. *Ind. Eng. Chem* **1947**, *39*, 427.
(2) Galindo, A.; Whitehead, P. J.; Jackson, G. *J. Phys. Chem. B* **1997**, *101*, 2082.
(3) Lee, J., D *A New Concise Inorganic Chemistry*, 3rd ed.; Van Nostrand Reinhold: Berkshire, 1977.
(4) Re, S. *J. Phys. Chem. A* **2001**, *105*, 9725.
(5) Pauling, L. *J. Chem. Educ.* **1956**, *33*, 16.
(6) Baburao, B.; Visco, D. P. *Ind. Eng. Chem. Res.* **2002**, *41*, 4863.
(7) Smith, C.; Visco, D. P. *J. Chem. Eng. Data* **2004**, *49*, 306.
(8) Vieweg, R. *Chem. Tech.* **1963**, *15*, 734.
(9) Miki, N.; Maeno, M.; Maruhashi, K.; Ohmi, T. *J. Electrochem. Soc.* **1990**, *137*, 787.
(10) Wierzchowski, S. J.; Kofke, D. A. *Ind. Eng. Chem. Res.* **2004**, *43*, 218.
(11) Simon, C.; Klein, L. M. *Chem. Phys. Chem* **2005**, *6*, 148.
(12) Lassonen, K.; Klein, L. M. *Mol. Phys.* **1996**, *88*, 135.
(13) Chipot, C.; Gorb, L. G.; Rivail, J. L. *J. Phys. Chem.* **1994**, *98*.
(14) Silanpaa, A. J.; Simon, C.; Klein, L. M.; Lassonen, K. *J. Phys. Chem. B* **2002**, *106*, 11315.
(15) Hannachi, Y.; Silvi, B.; Bouteiller, Y. *J. Chem. Phys.* **1991**, *94*, 2915.
(16) Kuo, J.-L.; Klein, M. L. *J. Chem. Phys.* **2004**, *120*, 4690.
(17) Chaban, G. M.; Gerber, B. R. *Spectrochim. Acta, A* **2002**, *58*, 887.
(18) Odde, S.; Mhin, B. J.; Lee, K. H.; Lee, H. M.; Tarakeshwar, P.; Kim, K. S. *J. Phys. Chem. A* **2006**, *110*, 7918.
(19) Odde, S.; Mhin, B. J.; Lee, H. M.; Kim, K. S. *J. Chem. Phys.* **2004**, *121*, 11083.
(20) Odde, S.; Mhin, B. J.; Lee, S.; Lee, H. M.; Kim, K. S. *J. Chem. Phys.* **2004**, *120*, 9524.
(21) Galindo, A.; Whitehead, P. J.; Jackson, G. *J. Phys. Chem. B* **1997**, *101*, 2082.
(22) Anderko, A. *Fluid Phase Equilib.* **1989**, *50*, 21.
(23) Anderko, A. *Fluid Phase Equilib.* **1991**, *65*, 89.
(24) Anderko, A. *Fluid Phase Equilib.* **1992**, *75*, 89.
(25) Visco, D. P.; Kofke, D. A. *Ind. Eng. Chem. Res.* **1999**, *38*, 4125.
(26) Redington, R. L. *J. Phys. Chem.* **1982**, *86*, 552.
(27) Zhao, Y.; Truhlar, D. G. *J. Phys. Chem. A* **2004**, *108*, 6908.
(28) Becke, A. D. *J. Chem. Phys.* **1996**, *104*, 1040.
(29) Adamo, C.; Barone, V. *J. Chem. Phys.* **1998**, *108*, 664.
(30) Hehre, W. J.; Ditchfield, R.; Pople, J. A. *J. Chem. Phys.* **1972**, *56*, 2257.
(31) Frisch, M. J.; Trucks, G. W.; Schlegel, H. B.; Scuseria, G. E.; Robb, M. A.; Cheeseman, J. R.; Montgomery, J., J. A.; Vreven, T.; Kudin, K. N.; Burant, J. C.; Millam, J. M.; Iyengar, S. S.; Tomasi, J.; Barone, V.; Mennucci, B.; Cossi, M.; Scalmani, G.; Rega, N.; Petersson, G. A.; Nakatsuji, H.; Hada, M.; Ehara, M.; Toyota, K.; Fukuda, R.; Hasegawa, J.; Ishida, M.; Nakajima, T.; Honda, Y.; Kitao, O.; Nakai, H.; Klene, M.; Li, X.; Knox, J. E.; Hratchian, H. P.; Cross, J. B.; Adamo, C.; Jaramillo, J.; Gomperts, R.; Stratmann, R. E.; Yazyev, O.; Austin, A. J.; Cammi, R.; Pomelli, C.; Ochterski, J. W.; Ayala, P. Y.; Morokuma, K.; Voth, G. A.; Salvador, P.; Dannenberg, J. J.; Zakrzewski, V. G.; Dapprich, S.; Daniels, A. D.; Strain, M. C.; Farkas, O.; Malick, D. K.; Rabuck, A. D.; Raghavachari, K.; Foresman, J. B.; Ortiz, J. V.; Cui, Q.; Baboul, A. G.; Clifford, S.; Cioslowski, J.; Stefanov, B. B.; Liu, G.; Liashenko, A.; Piskorz, P.; Komaromi, I.; Martin, R. L.; Fox, D. J.; Keith, T.; Al-Laham, M. A.; Peng, C. Y.; Nanayakkara, A.; Challacombe, M.; Gill, P. M. W.; Johnson, B.; Chen, W.; Wong, M. W.; Gonzalez, C.; Pople, J. A. *Gaussian 03*, Revision D.01; Gaussian, Inc.: Pittsburgh PA, 2003.
(32) Janzen, J.; Bartell, L. S. *J. Chem. Phys.* **1969**, *50*, 3611.
(33) Pine, A. S.; Howard, B. J. *J. Chem. Phys.* **1986**, *84*, 590.
(34) Howard, B. J.; Dyke, T. R.; Klemperer, W. *J. Chem. Phys.* **1984**, *81*, 5417.
(35) Pine, A. S.; Lafferty, W. J. *J. Chem. Phys.* **1983**, *78*, 2154.
(36) Andrews, L.; Bondybey, V. E.; English, J. H. *J. Chem. Phys.* **1984**, *81*, 3452.
(37) Michael, D. W.; Lisy, J. M. *J. Chem. Phys.* **1986**, *85*, 2528.
(38) Huisken, F.; Kaloudis, M.; Kulcke, A.; Laush, C.; Lisy, J. M. *J. Chem. Phys.* **1995**, *103*, 5366.
(39) Blake, T. A.; Sharpe, S. W.; Xantheas, S. S. *J. Chem. Phys.* **2000**, *113*, 707.
(40) Andrews, L.; Souter, P. F. *J. Chem. Phys.* **1999**, *111*, 5995.
(41) Quack, M.; Schmitt, U.; Suhm, M. A. *Chem. Phys. Lett.* **1993**, *208*, 446.
(42) Quack, M.; Schmitt, U.; Suhm, M. A. *Chem. Phys. Lett.* **1997**, *269*, 29.
(43) Quack, M.; Suhm, M. A. *Adv. Mol. Vibr. Collis. Dyn.* **1998**, *3*, 205.
(44) Rankin, K. N.; Boyd, R. J. *J. Comput. Chem.* **2001**, *22*, 1590.
(45) Del, Bene, J. E.; Person, W. B.; Szczepaniak, K. *J. Phys. Chem.* **1995**, *99*, 10705.
(46) Halkier, A.; Klopper, W.; Helgaker, T.; Jorgensen, P.; Taylor, P. R. *J. Chem. Phys.* **1999**, *111*, 9157.
(47) Rincon, L.; Almeida, R.; Garcia−Aldea, D.; Diez, y. R. H. *J. Chem. Phys.* **2001**, *114*, 5552.
(48) Hodges, M. P.; Stone, A. J.; Lago, E. C. *J. Phys. Chem. A* **1998**, *102*, 2455.
(49) Curtiss, L. A.; Blander, M. *Chem. Rev.* **1988**, *88*, 827.
(50) Gaw, J. F.; Yamaguchi, Y.; Vincent, M. A.; Schaefer, H. F.; III. *J. Am. Chem. Soc.* **1984**, *106*, 3133.
(51) Guedes, R. C.; do Couto, P. C.; Costa, Cabral, B. J. *J. Chem. Phys.* **2003**, *118*, 1272.
(52) Rincon, L.; Almeida, R.; Aldea, D. G. *Int. J. Quant. Chem.* **2004**, *102*, 443.
(53) Wierzchowski, S. J.; Fang, Z. H.; Kofke, D. A.; Tilson, J. L. *Mol. Phys.* **2006**, *104*, 503.
(54) Klopper, W.; Quack, M.; Suhm, M. A. *Chem. Phys. Lett.* **1996**, *261*, 35.
(55) Quack, M.; Suhm, M. A. *Theor. Chim. Acta* **1996**, *93*, 61.
(56) Diercksen, G. H. F.; Kraemer, W. P. *Chem. Phys. Lett.* **1970**, *6*, 419.
(57) Kollman, P. A.; Allen, L. C. *J. Chem. Phys.* **1970**, *52*, 5085.
(58) Schwenke, D. W.; Truhlar, D. G. *J. Chem. Phys.* **1985**, *82*, 2418.
(59) Latajka, Z.; Scheiner, S. *J. Comp. Chem.* **1987**, *8*, 663.
(60) Yarkony, D. R.; O'Neil, S. V.; Schaefer, H. F., III; Baskin, C. P.; Bender, C. F. *J. Chem. Phys.* **1974**, *60*, 855.
(61) Frisch, M. J.; Del Bene, J. E.; Binkley, J. S.; Schaefer, H. F., III. *J. Chem. Phys.* **1986**, *84*, 2279.
(62) Chase, M. W., Jr. *NIST-JANAF Thermochemical Tables*, 4th ed.; *J. Phys. Chem. Ref. Data. Monogr*. **1998**, 9.
(63) Dyke, T. R.; Howard, B. J.; Klemperer, W. *J. Chem. Phys.* **1972**, *56*, 2242.
(64) Kitaura, K.; Morokuma, K. *Int. J. Quantum Chem.* **1976**, *10*, 325.
(65) Karpfen, A. *Adv. Chem. Phys.* **2002**, *123*, 469.
(66) Ludwig, R. *Angew. Chem.* **2001**, *40*, 1808.

(67) Liu, S. Y.; Michael, D. W.; Dykstra, C. E.; Lisy, J. M. *J. Chem. Phys.* **1986**, *84*, 5032.
(68) Keutsch, F. N.; Cruzan, J. D.; Saykally, R. J. *Chem. Rev.* **2003**, *103*, 2533.
(69) Mrazek, J.; Burda, J. V. *J. Chem. Phys.* **2006**, *125*, 194518/1.
(70) Wales, D. J. Water Clusters. In *Encyclopedia of Computational Chemistry*; Schleyer, P. v. R., Allinger, N. L., Clark, T., Gasteiger, J., Kollman, P. A., Schaefer, H. F., Schreiner, P. R., Eds.; John Wiley and Sons: Chichester, U.K., 1998; Vol. 5, pp 3183.
(71) Mueller−Dethlefs, K.; Hobza, P. *Chem. Rev.* **2000**, *100*, 143.
(72) Ugalde, J. M.; Alkorta, I.; Elguero, J. *Angew. Chem.* **2000**, *39*, 717.
(73) Dyke, T. R.; Muenter, J. S. *J. Chem. Phys.* **1974**, *60*, 2929.
(74) Dyke, T. R.; Mack, K. M.; Muenter, J. S. *J. Chem. Phys.* **1977**, *66*, 498.
(75) Odutola, J. A.; Dyke, T. R. *J. Chem. Phys.* **1980**, *72*, 5062.
(76) Fraser, G. T. *Int. Rev. Phys. Chem.* **1991**, *10*, 189.
(77) Feller, D. *J. Chem. Phys.* **1992**, *96*, 6104.
(78) Pugliano, N.; Cruzan, J. D.; Loeser, J. G.; Saykally, R. J. *J. Chem. Phys.* **1993**, *98*, 6600.
(79) Pribble, R. N.; Zwier, T. S. *Science* **1994**, *265*, 75.
(80) Millot, C.; Soetens, J.−C.; Costa, M. T. C. M.; Hodges, M. P.; Stone, A. J. *J. Phys. Chem. A* **1998**, *102*, 754.
(81) Gregory, J. K.; Clary, D. C. *J. Phys. Chem. A* **1997**, *101*, 6813.
(82) Feyereisen, M. W.; Feller, D.; Dixon, D. A. *J. Phys. Chem.* **1996**, *100*, 2993.
(83) Xantheas, S. S. *J. Chem. Phys.* **1996**, *104*, 8821.
(84) Estrin, D. A.; Paglieri, L.; Corongiu, G.; Clementi, E. *J. Phys. Chem.* **1996**, *100*, 8701.
(85) Xantheas, S. S. *J. Chem. Phys.* **1994**, *100*, 7523.
(86) Scheiner, S. *Ann. Rev. Phys. Chem.* **1994**, *45*, 23.
(87) Xantheas, S. S.; Dunning, T. H., Jr. *J. Chem. Phys.* **1993**, *99*, 8774.
(88) Laasonen, K.; Parrinello, M.; Car, R.; Lee, C.; Vanderbilt, D. *Chem. Phys. Lett.* **1993**, *207*, 208.
(89) Chakravorty, S. J.; Davidson, E. R. *J. Phys. Chem.* **1993**, *97*, 6373.
(90) Millot, C.; Stone, A. J. *Mol. Phys.* **1992**, *77*, 439.
(91) Smith, B. J.; Swanton, D. J.; Pople, J. A.; Schaefer, H. F.; III;, Radom, L. *J. Chem. Phys.* **1990**, *92*, 1240.
(92) Honegger, E.; Leutwyler, S. *J. Chem. Phys.* **1988**, *88*, 2582.
(93) Schutz, M.; Rauhut, G.; Werner, H.-J. *J. Phys. Chem. A* **1998**, *102*, 5997.
(94) Bentwood, R. M.; Barnes, A. J.; Orville-Thomas, W. J. *J. Mol. Spectrosc.* **1980**, *84*, 391.
(95) Del Bene, J.; Pople, J. A. *J. Chem. Phys.* **1970**, *52*, 4858.
(96) Masella, M.; Flament, J.-P. *J. Chem. Phys.* **1999**, *110*, 7245.
(97) Masella, M.; Flament, J. P. *J. Chem. Phys.* **1997**, *107*, 9105.
(98) Kim, K. S.; Dupuis, M.; Lie, G. C.; Clementi, E. *Chem. Phys. Lett.* **1986**, *131*, 451.
(99) Schütz, M.; Klopper, W.; Lüthi, H.-P.; Leutwyler, S. *J. Chem. Phys.* **1995**, *103*, 6114.
(100) Maheshwary, S.; Patel, N.; Sathyamurthy, N.; Kulkarni, A. D.; Gadre, S. R. *J. Phys. Chem. A* **2001**, *105*, 10525.
(101) Mhin, B. J.; Kim, H. S.; Kim, H. S.; Yoon, C. W.; Kim, K. S. *Chem. Phys. Lett.* **1991**, *176*, 41.
(102) Tsai, C. J.; Jordan, K. D. *Chem. Phys. Lett.* **1993**, *213*, 181.
(103) Pedulla, J. M.; Vila, F.; Jordan, K. D. *J. Chem. Phys.* **1996**, *105*, 11091.
(104) Mhin, B. J.; Kim, J.; Lee, J. Y.; Kim, K. S. *J. Chem. Phys.* **1994**, *100*, 4484.
(105) Kim, K.; Jordan, K. D.; Zwier, T. S. *J. Am. Chem. Soc.* **1994**, *116*, 11568.
(106) Lee, C.; Chen, H.; Fitzgerald, G. *J. Chem. Phys.* **1994**, *101*, 4472.
(107) Kim, J.; Kim, K. S. *J. Chem. Phys.* **1998**, *109*, 5886.
(108) Kryachko, E. S. *Int. J. Quantum Chem.* **1998**, *70*, 831.
(109) Kryachko, E. S. *Chem. Phys. Lett.* **1999**, *314*, 353.
(110) Tissandier, M. D.; Singer, S. J.; Coe, J. V. *J. Phys. Chem. A* **2000**, *104*, 752.
(111) Chesnut, D. B. *J. Phys. Chem. A* **2002**, *106*, 6876.
(112) Losada, M.; Leutwyler, S. *J. Chem. Phys.* **2002**, *117*, 2003.
(113) Kabrede, H.; Hentschke, R. *J. Phys. Chem. B* **2003**, *107*, 3914.
(114) Upadhyay, D. M.; Shukla, M. K.; Mishra, P. C. *Int. J. Quantum Chem.* **2001**, *81*, 90.
(115) Jensen, J. O.; Krishnan, P. N.; Burke, L. A. *Chem. Phys. Lett.* **1995**, *241*, 253.
(116) Kryachko, E. S. *Chem. Phys. Lett.* **1997**, *272*, 132.
(117) Kim, J.; Majumdar, D.; Lee, H. M.; Kim, K. S. *J. Chem. Phys.* **1999**, *110*, 9128.
(118) Kim, J.; Mhin, B. J.; Lee, S. J.; Kim, K. S. *Chem. Phys. Lett.* **1994**, *219*, 243.
(119) Jensen, J. O.; Krishnan, P. N.; Burke, L. A. *Chem. Phys. Lett.* **1995**, *246*, 13.
(120) Kim, J.; Mhin, B. J.; Lee, S. J.; Kim, K. S. *Chem. Phys. Lett.* **1994**, *219*, 243.
(121) Belair, S. D.; Francisco, J. S. *Phys. Rev. A* **2003**, *67*, 063206.
(122) Legon, A. C.; Millen, D. J.; North, H. M. *Chem. Phys. Lett.* **1987**, *135*, 303.
(123) Bevan, J. W.; Kisiel, Z.; Legon, A. C.; Millen, D. J.; Rogers, S. C. *Proc. R. Soc. London, Ser. A* **1980**, *372*, 441.
(124) Nirmala, V.; Kolandaivel, P. *Z. Phys. Chem* **2004**, *218*, 327.
(125) Diri, K.; Myshakin, E. M.; Jordan, K. D. *J. Phys. Chem. A* **2005**, *109*, 4005.
(126) Xantheas, S. S. *Int. Rev. Phys. Chem.* **2006**, *25*, 719.